Dear Dr. Alex,

We have responded to all the comments by the referees. The advance and retreat solutions have been computed with a 0.5 km long spatial step as suggested by a referee. The grounding line (GL) position does not move very much even compared to the 4 km step but the velocity is much better resolved at the GL with the finer mesh. We write in the title and Introduction that the scheme is tested in two dimensions but it can be extended to three dimensions as sketched in Discussion. The GL is found by a first order accurate numerical method which is consistent with all other first order approximations in the finite element method used in this paper and Elmer/ICE. We review other subgrid methods for other models which all are simplifications of the full Stokes (FS) model. The FS model is needed at the GL to capture the vertical stress component there. We refer to papers with arguments supporting that view. The difficulty with the FS equations compared to e.g. the SSA equations is that the vertical velocity in FS moves the base of the floating ice and Archimedes' flotation criterion is not valid at the GL. The vertical velocity introduces another boundary condition on the velocity in the normal direction of the grounded ice which disappears after the GL. The main result is that by subgrid modeling we obtain an accuracy for the GL position comparable to previously published results using more than 20 times larger spatial steps (25-200 m).

We really appreciate your help.

Best wishes,

Gong Cheng, Per Lötstedt and Lina von Sydow

Response to Anonymous Referee #1

March 10, 2020

The manuscript aims to present a numerical scheme to deal with the friction inside elements partly floating in a (full-)Stokes formulation for the marine ice sheet simulation. The formulation and results are carried out in a 2D vertical domain, and possible extension to 3D domain is discussed. The reviewed version presents the corrections asked in the first review, mainly in the technical part (methods). The Introduction was changed, but additional "polishing" is needed before publishing. No additional simulations were carried out, and the presentation of the results was not modified

General comments

- The numerical scheme is better presented in this new version, although some minor corrections should be done. See specific comments.

  Response: The correction has been made.

- With the results presented along the manuscript it is hard to analyze the convergence (and consistency) of the subgrid scheme proposed. There is no convergence rate analysis or comparison with the cited reference work (Gagliardini et al., 2016). I strongly recommend additional simulations (mesh resolutions equal to 500 m and 250 m) and a comparison with the results from Gagliardini et al. (2016), mainly in terms of GL position against mesh resolution.

  Response: Additional simulation with 500 m mesh resolution has been added, and it is compared with the results in Gagliardini et al. (2016), shown in a new Fig. 6.

- The overall explanation of the subgrid scheme was improved, which helps the reproducibility of the results.

  Response: Thanks for the comments. We improved the subgrid section a bit more according to the specific comments.

- The Introduction section must be improved yet. The reading is not smooth yet, and additional polishing is needed to make the reading "pleasant" enough for a scientific/technical paper.

  Response: The Introduction has been modified.

- The citation style along the manuscript was corrected, but there are still corrections in some parts. See specific comments.

  Response: The corrections have been made.

Specific comments

- line 77: "for modeling of the flow" => "for modeling the flow"

  Response: The correction has been made.

- line 78: "These nonlinear" => "The nonlinear"

  Response: The correction has been made.

- line 102: "β" => "$\beta(\geq 0)$"

  Response: The correction has been made.

- line 117: $z_b < 0$ => $z_b > b(x)$

  Response: The correction has been made.

- line 119: "The solution close to the grounding line" => "A first order solution close to the grounding line" or "A solution close to the grounding line from the boundary layer theory" or "A boundary layer' solution close to the grounding line". Note that this solution is based on a linear Stokes problem (i.e., n = 1 in Glen's flow law).

  Response: The headline has been changed.

- line 121: "(Schoof, 2011)" => "Schoof (2011)"

  Response: The correction has been made.

- line 123: "u" => "the ice velocity u"

  Response: The correction has been made.

- line 124: "ice surface slope is continuous": are you referring to slope or just the ice surface? Does this proposition come from Schoof (2011)? Also, why this is important/relevant for the subgrid scheme used here?

  Response: These are the words used by Schoof. We could have written 'the space derivative of the height of the ice is continuous' but chose to do it in this way. A reference to Schoof's paper is included. The section describes the analytically derived properties of the solution close to the GL. We show later how our treatment of the GL agrees to first order with the analysis by Schoof.

- line 128: "(Durand et al., 2009a)" => "Durand et al. (2009a)"

  Response: The correction has been made.

- line 129: "(Schoof, 2011, Ch. 4.3)" => "Schoof (2011, Sect. 4.3)"

  Response: The correction has been made.

- line 129: "parameters" => "parameters,"

  Response: The correction has been made.

- line 133: "variables satisfy" => "variables satisfy (Schoof, 2011)" (if the citation is right)

  Response: The correction has been made.

- line 142: "(Norwicki and Wingham, 2008)" => "Norwicki and Wingham (2008)"

  Response: The correction has been made.

- line 143: "original variables": what does it mean?

  Response: The original, unscaled variables is what it is meant. The words are removed.

- line 149: The definition of "k" and "k^*" is weird. Why does the approximation space depend on the Glen's flow law? Are these not referred to the polynomial order of the space? Please, check the definition and notation of these spaces.

  Response: We now tell where in the three theoretical papers the functional spaces are defined. They are the same in all the three papers. A short discussion is found in the paper by Jouvet and Rappaz(2011). We do not delve into this issue in details in our paper.

- line 152: Please, change the citation style here

  Response: The correction has been made.

- line 156: the form "$b(v, q)$" is not defined here (although it follows $b(u, p)$)

  Response: As $b(\cdot, \cdot)$ defines a bi-linear form, we think that $b(v, p)$ follows from the definition of $b(u, q)$ in Eq (14).

- line 156: where is σ_{nt} in the expressions? Please, check the forms B_Γ; and B_N

  Response: σ_{nt} is now in the definition of B_Γ. On Γ_{bg}, σ_{nt} is replaced by the slip boundary condition $-\beta u$. On Γ_{bf}, $\sigma_{nt} = 0$.

- line 156: How the forcing term $F(v)$ is numerically considered in the element crossed by the grounding line? There is no mention of this along the text.

  Response: The forcing term is split into the interior term F and the boundary term F_Γ. A sentence is added to explain the boundary term $F_\Gamma(v)$. The integration of F_Γ is shown Eqs (15) and (30) in the numerical Section 4.

- line 171: Do you also split the in integral of the forcing term $F(v)$?

  Response: As explained above, the term $F(v)$ is from the gravitational force which is smooth over the GL. The boundary term F_Γ is from the ice-ocean interface and is integrated partially on the floating ice as in Eqs (15) and (30).

- line 173: Eq. (15): the forms B_Γ; and B_N are already integrated. Please, fix the notation here.

  Response: This is corrected now.

- line 173: Eq. (15): where is the σ_{nt} ? Please, check the forms here.

  Response: As explained above (line 156), σ_{nt} is replaced by the slip boundary condition in B_Γ on Γ_{bg} and vanishes due to the ice-ocean interface condition on Γ_{bf}.

- line 173: Eq. (15): the forcing $p_w n \cdot v$ is considered here, but is it included in the stiff matrix? Please, could you make it clearer?

  Response: No, $p_w n \cdot v$ is not included in the stiffness matrix because it does not depend on u.

- lines 175-177: "With a strong formulation ... into account". This is phrase is not clear. I don't understand why strong formulation is mentioned here.

  Response: We mean the strong formulation of the boundary condition. We have added more explanation after Eq (15).

- line 177: "no basis functions satisfies ...". I am not sure if this is true. There are lots of FEM schemes where the discontinuity is well accommodated (e.g., xFEM, CutFEM, etc). The phrase is only true if the standard FEM is used, and no specific refinement is made in the element crossed by the grounding line (as is the case of this paper).

  Response: Yes, this is correct. We remark that we use the standard FEM basis functions in Elmer/ICE after Eq (28).

- lines 185-186: what does "along the slope" mean?

  Response: It is changed to "along the ice base".

- line 195: "The nonlinear equations ..." => "The nonlinear equations, Eq. (14), ..."

  Response: The correction has been made.

- line 197: "timestep" => "time step" (and elsewhere)

  Response: The correction has been made.

- line 198: "nonlinear iterations" => "nonlinear iterations (Picard)"

  Response: The correction has been made.

- Algorithm 1: All grounded nodes are marked as "GL nodes"? Please, could you make it clearer along the text? Also, check the text punctuation in Algorithm 1

  Response: The term "GL nodes" is only used in Algorithm 1. A new sentence is added before Algorithm 1 explaining that it will be in one element. Some text punctuation is added.

- Algorithm 2: please, check the text punctuation in Algorithm 2

  Response: The correction has been made.

- line 208: "A stability problem" => "A numerical stability problem"

  Response: The correction has been made.

- line 208: "(Durand et al., 2009a)" => "Durand et al. (2009a)" Same in lines 209, 238.

  Response: The correction has been made.

- line 215: "is updated implicitly": is p_w also considered in the forcing term of Eq. (14)? Could you make it clearer?

  Response: Yes, the p_w in Eq (14) is udated implicitly. A few words after Eq (23) explain this.

- line 221: note that n was used before with another meaning

  Response: All the terms with n for the time discretization are changed to ℓ.

- line 242: "(Seroussi et al., 2014)" => "Seroussi et al., (2014)". The same for Schoof citation

  Response: The correction has been made.

- line 249: "(11)" => "Eq. (11)"

  Response: The correction has been made.

- line 251: please, change the citation style here

  Response: The correction has been made.

- line 251: "analytical solution": which one? From Schoof 2011's paper? Same in line 254. Note that if it is from Schoof (2011), it is based on a linear Stokes problem $n = 1$ (Glen's flow law).

  Response: It is the analytical solution to the FS equation, without any approximation or simplification. This is now more clearly stated.

- line 258: "between" => "between any"

  Response: The correction has been made.

- line 261: "basal surface of the ice" => "ice base"

  Response: The correction has been made.

- line 266: "external forces" => "external forces and boundary conditions" (maybe?)

  Response: The correction has been made.

- line 267: "geometrically grounded": how is the element identified as geometrically grounded or geometrically floating, in the numerical framework? Could you make it clearer along the text?

  Response: A reference to Algorithm 1 is added to clarify this.

- line 269: "(Gagliardini et al., 2016)" => "Gagliardini et al. (2016)"

  Response: The correction has been made.

- line 270: please, delete the extra "the"

  Response: The correction has been made.

- line 271: "fine mesh" => "fine mesh resolution (< 100 m)" (maybe?)

  Response: The correction has been made.

- Fig. 2 and Fig. 3: "net forces" => "net forces in the vertical direction" (please, check also the text)

  Response: The correction has been made.

- Eq. (27): $\chi(x_i) = 0$, right? Or this is not zero in the numerical solution? Please, could you make it clearer along the text?

  Response: The extrapolated χ and $\tilde{\chi}$ satisfy $\chi(x_i) > 0$ and are better explained now in Sect 4. A modification of them is necessary at x_i.

- line 280: "best numerical approximation". I don't know if "best" is the word here. Maybe mentioning that it is in the same order of the framework/scheme/approximation space

  Response: We have written about it below Eq (29).

- line 284-285: "Considering ... always stays": maybe this phrase is unnecessary; even the numerical GL position stays on bedrock

  Response: We have removed the sentence. It follows from the interpolation in Eq (28) that the numerical x_{GL} stays on the element boundary.

- line 293: "bottom surface" => "ice base"

  Response: The correction has been made.

- line 296: please, delete "Then"

  Response: The correction has been made.

- line 297: “(Seroussi et al., 2014)” => “Seroussi et al., (2014)”. Same in line 299

  Response: The correction has been made.

- line 299: “condition” => “condition, respectively”

  Response: The correction has been made.

- line 299: “reasonable resolution” => “reasonable numerical accuracy”

  Response: The correction has been made.

- line 300: “required” => “used”. The integration points are defined over the GL element, right? And the step function makes the work of selecting the area to be integrated, right? Then, note that, depending on the situation, even a tenth order could not be enough to carry out the integration with enough numerical accuracy (as is the SEP2 method of Seroussi et al., 2014, where the distribution of the integration points follows the grounding line position inside the GL element). Besides that, the approach used here seems reasonable, and it is easier to be implemented in comparison to SEP2-type scheme.

  Response: Changed. Yes, with this integration scheme, a tenth order polynomial is used to approximate the step function.

- line 302: “fully on the ground”: geometrically, right?

  Response: Yes, it is changed to “fully geometrically on the ground”.

- line 304: “basal surface” => “ice base”

  Response: The correction has been made.

- line 307: “fully grounded” => “fully geometrically grounded” (maybe?)

  Response: The correction has been made.

- line 308: “boundary elements” => “basal elements” (maybe?)

  Response: The correction has been made.

- line 311: “floating elements” => “fully geometrically floating elements” (maybe)

  Response: The correction has been made.

- line 313: “grounded” => “geometrically grounded” (maybe)

  Response: The correction has been made.

- line 313: “analytical solution”: maybe “numerical solution”? It is not clear what you meant here

  Response: The analytical solution to the FS.

- line 315: “3” => “Fig. 3”

  Response: The correction has been made.

- Eq. (29): check the notation of the forms B_Γ and B_N. Also, there is no σ_{nt} here

  Response: The notation has been changed and σ_{nt} is replaced by $-\beta(t \cdot u)(t \cdot v)$ as in Eq (14).

- lines 319-320: How are the phases (advance or retreat) defined? Comparing with previous (last time step) GL position? Please, could you make it clearer?

  Response: This is clarified now in Sect 4.

- Algorithm 3: please, check the text punctuation in Algorithm 3

  Response: The correction has been made.

- line 326: in the calculation of $\tilde{\chi}, p_w$ is kept constant, right? Could you please make it clearer?

  Response: Yes, it is fixed. A new sentence is added.

- line 330: “(Gagliardini et al., 2016)” => Gagliardini et al., (2016)”. The same in lines 331, 367, 369, 370, 372, 397, 398

  Response: The correction has been made.

- line 342: “both for” => “for both”

  Response: The correction has been made.

- line 344: please, correct the citation style

  Response: The correction has been made.

- line 352: “(van Dongen et al., 2018)” => “van Dongen et al. (2018)”

  Response: The correction has been made.

- line 357: “(Schoof, 2011)” => “Schoof (2011)”

  Response: The correction has been made.

- line 357: “represented” => “captured

  Response: The correction has been made.

- line 359: “Seroussi et al (Seroussi et al., 2014)” => Seroussi et al. (2014) (maybe?)

  Response: The correction has been made.

- Fig. 6: Note that the GL is close to a node. I suspect the same is observed for the other resolutions (2 and 4 km). So, the GL position also depends on the distribution of the nodes in 1D.

  Response: Yes, it depends on the node positions and the mesh size but that is true also for the smooth solution away from the GL. The solution is mesh dependent. The GL position between the nodes is mentioned in the end of Results.

- line 363: "floatation criterion" => "hydrostatic floatation criterion"

  Response: The correction has been made.

- line 372: "asymptote" => "convergence asymptote" (maybe?)

  Response: The correction has been made.

- lines 374-375: "but the numerical solution of the velocity field, pressure as well as the two free surfaces are still determined by the coarse mesh ...": note that small bedrock features impact the GL dynamics, and they are important in short time scale simulations (decades). In general, mesh resolution equal to 500 m is required to capture these bedrock features near the GL. Also, from figures 6 and 7, there are expressive changes in the fields near the GL (thickness, surface, horizontal and vertical velocities). These changes are only "well" captured with enough mesh resolution (¡1 km or less). Besides that, no error estimator was used here; therefore, the term "determined" doesn't fit here. The subgrid scheme tends to accelerate the rate of convergence in comparison to NSEP-type schemes (by decreasing the numerical error of one source, the boundary condition at the base), but relatively fine mesh resolution (I would say 500 m) is yet required around the GL to numerical error control (from other sources, e.g., bedrock geometry, intrinsic solutions variations around GL, effect of ocean-induced basal melting, etc).

  Response: We have new Figs. 7 and 8 with 500 m resolution. Except for the GL position, the solution around the GL looks very much the same (excluding details) as the solution with 1 km resolution. Larour et al(2019) say that 1 km is satisfactory. It seems as if 500 m is sufficient. We have added one new reference where the sensitivity to the base friction and the bedrock geometry is investigated. The sensitivity increases the closer the surface observation of velocity and height is to the GL.

- line 377: "following way" => "following way (considering linear Lagrange functions)" (maybe?)

  Response: The correction has been made.

- line 382: "An alternative to a subgrid scheme is to introduce dynamic adaptation of the mesh": I don't think mesh adaptation is an alternative, strictly speaking. They are complementary to each other. The subgrid scheme tends to decrease the error on the boundary condition, accelerating the rate of convergence (ideally); the mesh adaptation helps save computation effort, since enough mesh resolution (500 m) is needed around the GL. They can (should) be used together, indeed.

Response: We have rewritten the paragraph now discussing static and dynamic adaptation and subgrid modeling.

- line 383: please, correct the citation style here

  Response: The correction has been made.

- line 386: "shorter timesteps are necessary for stability when the mesh size is smaller in a mesh adaptive method" => "shorter time steps are necessary for numerical stability in dynamic mesh adaptation schemes". Note that it depends on the numerical implementation; some schemes are more stable than others.

  Response: The correction has been made.

- line 387: "Introducing a time dependent mesh adaptivity into an existing code requires a substantial coding effort and will increase the computational work considerably. Subgrid modeling is easier to implement and the increase in computing time is small." I don't totally agree here. Yes, mesh adaptivity is a substantial coding effort, and there are drawbacks in scalability. But at the end, the computational effort is (or should be) much less in comparison to a fine uniform mesh. The improvement of a subgrid scheme for the basal condition (friction) makes the 25 m-mesh resolution requirement to a 500 m-mesh resolution requirement. But yet, a 500 m-mesh resolution is expressively fine in comparison to a typical horizontal scale of ice sheets (order of 1,000 km). A static mesh adaptation (performed during the domain discretization) could be used instead of dynamic mesh adaptation (considering the GL will not migrate beyond the adapted/refined region). For short-term simulations (decades) this is feasible, but this is not totally true for paleo-ice sheets simulations. Therefore, using subgrid scheme with dynamic mesh adaptation should work properly (in the sense of convergence of the GL dynamics with reduced computational effort).

  Response: The paragraph has been rewritten as described above taking these comments into account.

- lines 390-392: "A subgrid scheme ... (Feldmann et al., 2014)": this phrase could be migrated to the discussion part. Also, correct the citation style here.

  Response: We have decided to keep the work by other researchers on subgrid schemes in Conclusions to contrast them to our work.

- line 395: "function $\chi(x)$" => "function $\chi(x)$ based on a first order approximation of the basal stress balance" (maybe?) Again, note that the solution from Schoof (2011) considers $n = 1$ (Glen's flow law), as you have well pointed along the text.

Response: The functions $\chi(x)$ and $\tilde{\chi}(x)$ are nonlinear. With the FEM discretization and linear Lagrange element we use, they are piecewise linear in x. This is remarked in Sect 4 now. In an expansion in small parameters and taking the first order approximation for $n = 1$ by Schoof we obtain χ_a which is close to our linear approximation.

- line 396: "is modified" => "is modified to accommodate the discontinuities in the boundary conditions"

  Response: The correction has been made.

- line 399: "Solving for ... GL position": I think this phrase could be deleted.

  Response: The correction has been made.

Response to Anonymous Referee #2

March 11, 2020

Major concerns

1. As clearly illustrated in the paper (Section 2.4, and many other places), the authors are using a first-order approximation to determine the location of the grounding line. Thus, I don't quite understand why they call it a "full Stokes subgrid scheme"?

   Response: The χ and $\tilde{chi}$ functions in Eqs (27) and (29) that we use to determine the GL position are nonlinear. After FEM discretization with the linear Lagrange element, they vary linearly in x over the GL element. These are the χ-functions that we have access to. We write about this in a revised Sect. 4. The linear interpolation to find x_{GL} is consistent with the level of approximation by FEM. The discussion in Sect. 2.4 is there only to lend analytical support and inspiration to our choice of χ. We still think that our method is a subgrid scheme for the FS equations.

2. In Elmer/Ice, originally, the location of the grounding line is decided by comparing the water pressure (p_w) and the normal stress (tau; which can be determined from the Stokes solution) at each node ($N = p_w - \tau$). We can tell which node is floating or grounded by looking at the sign of N. Note that Elmer/Ice uses nodal force and contact force, instead of the actual water pressure and normal stress. Therefore, if we consider a 2D case, I guess it would still be possible to estimate the exact grounding line location by simply interpolating the N values at two neighboring nodes. Did the authors test it and then decide to go for their first-order method? If yes, what is the difference between these two methods?

   Response: For linear Lagrange elements used in this paper and Elmer/ICE, the pressure and stress can be represented by the nodal force and contact force together with the basis functions. If $N = \tau_{\mathbf{nn}} - p + p_w$, this paper follows the same criteria as Elmer/ICE to determine the grounded and floating nodes. Indeed, the GL position is determined by the linear interpolation of the N value. However, notice that a naive linear interpolation will not give a good estimate of the GL position, simply because $N = 0$ on any floating nodes. That is why we introduce the function $\tilde{\chi}$ and use it to determine the GL instead.

3. If the author cannot provide the sub-grid results of 3D experiments (i.e., MISMIP3d), I would question the applicability of this 2D scheme in 3D cases. I agree the 2D results are still valuable in some senses, but for a complete and thorough evaluation of this first-order sub-grid scheme, I would suggest the authors do the MISMIP3d tests before its final publication. However, if the editor and other reviewers feel the 2D experiments are sufficient to prove its applicability, I would strongly suggest they remove all 3D discussions in the paper, and explicitly demonstrate that it is a 2D scheme in the title and elsewhere in the manuscript. A possible title would be "A two-dimensional first-order subgrid scheme for simulation of grounding line migration in ice sheets using Elmer/ICE (v8.3)". By that it is safe to limit this paper in 2D discussion.

   Response: We keep the description of a possible extension to 3D in Discussion but add 2D in the title and stress 2D in Introduction. See also the response to Major concern 1.

4. I am confused about the subgrid scheme, i.e., Eq (29). According to Line 267-268, the GL element is referred to the element that is partially grounded and partially floating. If it is true, then the Nitsche step function in Eq (29) should be 0, according to Line 301-302, "it is only imposed on the element which is fully on the ground" (I interpret it as "fully grounded"), and the lower panels in Fig. 2 and 3. Then, the right hand side of Eq. (29) is

$$\int_{\varepsilon_i} \mathcal{H}_\beta \beta \mathbf{u} \cdot \mathbf{v} + p_w \mathbf{n} \cdot \mathbf{v} \mathrm{d}s$$

   This is different from Eq. (15) where the water pressure term is integrated partially from x_{GL} to x_i, instead of over the whole GL element. Also, I still don't follow where the friction step function of 1 / 2 is from. In the previous first round of the review, there was already a question about this, as it looks like a smoothing function than a partial integration using JUST the integration points in the grounded portion of the GL element. I don't get useful answers from the authors' response to this point.

   Response: Corrections are made in (15) and (30). $B_\mathcal{N} + B_\Gamma$, F and F_Γ are separated. There are actually two levels of smoothing: the high order integration scheme in the subgrid model smooths the changes of the boundary conditions jumping from one node to another (between Eq. (5) and (6)); the 1/2 coefficient smooths the jump at the step function. The high order scheme acts on the friction law at the mesh size level with the step function $\mathcal{H}_\beta$ and the 1/2 coefficient acts at the integration points level to smear out the rapid change of the step function.

Minor points

The abstract needs improvements. The abstract should cover the key points of the paper and the current version is still a bit ambiguous. My suggestion is it should at least cover the details of the improvements of the sub-grid method, compared to old model results.

Response: Two sentences have been added to Abstract.

The flow of the introduction section needs further care. For example, in the paragraph Line 28-34, the authors discussed a bit of different "model equations" (which looks a bit odd), and then in the paragraph Line 46-54, the authors discussed about different lower order models again. Would be nice to put them together so that the readers can easily follow the authors' logic here? Another example is that, in the paragraph Line 46-54, the authors discussed the sub-grid scheme and said "the purpose of a subgrid scheme is to avoid such fine meshes", and then in the next paragraph there is a similar sentence "Our subgrid scheme is aiming at improving the accuracy in GL simulations for a static mesh". It would be great if the authors make further organization for the introduction section.

Response: Introduction has been reorganized and partly rewritten.

I don't think the citation style is correct. For example, Line 14, "It is shown in (Kingslake et al., 2018)" should be "It is shown in Kingslake et al. (2018)". Similar mistakes should be corrected all over the whole paper.

Response: The corrections have been made.

- Line 12: remove "be able"

  Response: The correction has been made.

- Line 13: change "sea" to "ocean"

  Response: The correction has been made.

- Line 15: "km" $->$ "kilometers"

  Response: The correction has been made.

- Line 18: The ice flow is dominated by vertical shear only when the basal friction is large.

  Response: This is added now.

- Line 20: Any references for "gradual change of the stress field"?

  Response: We refer to Schoof 2011.

- Line 23: "interaction" $->$ "coupling"

  Response: The correction has been made.

- Line 28: this sentence is unclear to me. I guess the authors try to say that different ice sheet models can generate different GL locations, which also depends on basal friction and some other numerical parameters. But it reads awkward.

  Response: We have separated the model and numerical method in this statement. The sentence is rewritten.

- Line 31-32: "ice equations such as FS and SSA" is right. We can't say "equations such as Full Stokes and Shallow Shelf Approximation".

  Response: We have rewritten the sentence.

- Line 51-52: Need details of the subgrid modeling in Cornford et al., 2016

  Response: Details have been included.

- Line 53-54: I suggest to remove the sentence "The purpose of ..."

  Response: It has been removed.

- Line 56: the sentence "Since the GL moves" duplicates with a similar sentence above

  Response: The correction has been made.

- Line 77: I would suggest use "2D ice domain" to replace "2D vertical ice"

  Response: In the first round of referee reports, one referee suggested the phrase '2D vertical ice' and we keep it like that.

- Line 86: in Eq (1), g is a vector, not its z component.

  Response: The correction has been made.

- Line 87: Change the sentence "The rate factor..." to "The viscosity (η) is a function of the rate factor A(T). T is the ice temperature."

  Response: The correction has been made.

- Line 91: "vector t, see Fig. 1" $->$ "vector t (see Fig. 1)"

  Response: The correction has been made.

- Line 91: "In the 2D vertical case" $->$ "For the 2D ice domain", and similarly in the following

  Response: See the response to line 77 above.

- Line 106: GL is the boundary (xGL, yGL) between ...

  Response: As defined in the text and shown in Fig. 1, the coordinate system in 2D is the $x-z$ plane. So, this should be (x_{GL}, z_{GL}).

- Line 108: "and g is ..." is a repeat of the description of g in Eq (1).

  Response: Changed. g is the vertical component of $\mathbf{g}$.

- Line 128: "as observed also" $->$ "as also observed"

  Response: The correction has been made.

- Line 136: On the grounded ice domain, we have ...

  Response: The correction has been made.

- Line 152, switch the order of references according to the year.

  Response: The correction has been made.

- Line 261-262: "by" $->$ "as"

  Response: The correction has been made.

- Line 264-265: at the node xi

  Response: The correction has been made.

- Figure 2: in the lower panel, why is the beta 1 / 2 at $[x_{GL}, x_i]$ where the ice is floating?

  Response: We have explanation in the paragraph preceding Eq (30) and in the response to Major concern 4.

- Line 292-294: The sentence "Moreover, this correction ... as discussed in Sect 3.3" is hard to understand. Can the authors provide more details/explanations? From my understanding, if we don't use a sub-grid scheme, wouldn't it be a slower advance?

  Response: Sect 4 with the definitions of χ and $\tilde{\chi}$ is rewritten with better explanations.

- Line 298: "slip boundary" $->$ "grounded boundary"

  Response: The 'slip boundary condition' refers to the boundary conditions of Γ_{bg} as defined in Eq. (5) which . We keep it as it is.

- Line 302: add comma after "On the contrary"

  Response: The correction has been made.

  There were no more comments after line 302 in the referee report we received.

A full Stokes subgrid scheme in two dimensions for simulation of grounding line migration in ice sheets using Elmer/ICE (v8.3)

Gong Cheng[1], Per Lötstedt[1], and Lina von Sydow[1]

[1]Department of Information Technology, Uppsala University, P. O. Box 337, SE-75105 Uppsala, Sweden

Correspondence: Gong Cheng (cheng.gong@it.uu.se)

Abstract. The full Stokes equations are solved by a finite element method for simulation of large ice sheets and glaciers. The simulation is particularly sensitive to the discretization of the grounding line which separates the ice resting on the bedrock and the ice floating on water and is moving in time. The boundary conditions at the ice base are enforced by Nitsche's method and a subgrid treatment of the element in the discretization with the grounding line. Simulations with the method in two dimensions for an advancing and a retreating grounding line illustrate the performance of the method. The computed grounding line position is compared to previously published data with a fine mesh. Similar results are obtained using subgrid modeling with more than 20 times coarser meshes. It is implemented in the two dimensional version of the open source code Elmer/ICE.

1 Introduction

~~Simulation with ice sheet models~~

1.1 Ice sheet dynamics, sea-level rise, and grounding line migration

Simulation of ice sheet dynamics is a tool to assess the future sea-level rise (SLR) due to melting of continental ice sheets and glaciers (Hanna et al., 2013) and to reconstruct the ice sheets of the past ~~(DeConto and Pollard, 2016; Stokes et al., 2015)~~ (Stokes et al., 2015; DeConto and Pollard, 2016) for comparison with measurements and validation of the models. ~~In the models, the~~ The predictions are particularly sensitive to the ~~numerical treatment~~ position of the grounding line (GL) ~~(Durand and Pattyn, 2015). The GL is~~ and its numerical treatment (Durand and Pattyn, 2015; Konrad et al., 2018), the line where the ice sheet leaves the solid bedrock and becomes an ice shelf floating on water driven by buoyancy. ~~It is important to know the GL position to be able to quantify the ice discharge into the sea and as an indicator of ice sheet advances or retreats (Konrad et al., 2018).~~

The distance that the GL moves may be long over palaeo time scales. ~~It is shown in (Kingslake et al., 2018)~~ In Kingslake et al. (2018) it is shown that the GL has retreated several hundred ~~km~~ kilometers in West Antarctica during the last 11,500 years and then advanced again after the isostatic rebound of the bed. The sensitivity, long time intervals, and long distances require a careful treatment of the GL and its neighborhood by the numerical method to discretize the ~~model equations .~~equations modeling the ice sheet dynamics. In this paper, we develop an accurate and efficient method for such problems.

1.2 Model equations

When the ice rests on the ground and is affected by frictional forces on the bed, the ice flow is dominated by vertical shear stresses ~~. The~~ when the basal friction is large. On the other hand, when the ice is floating on water, it is the longitudinal stress gradient that controls the flow of the ice~~floating on water~~. The GL is in the transition zone between these two types of flow with a gradual change of the stress field (Schoof, 2011).

The most accurate ice model in theory is based on the full Stokes (FS) equations. A simplification of the FS equations by integrating in the depth of the ice is the shallow shelf (or shelfy stream) approximation (SSA) (MacAyeal, 1989). It is often used for simulation of the ~~interaction~~ coupling between a grounded ice sheet and a marine ice shelf. In the zone between the grounded ice and the floating ice, it is necessary to use the FS equations ~~(Docquier et al., 2011; Schoof, 2011; Schoof and Hindmarsh, 2010; Wilchinsky a~~ (Wilchinsky and Chugunov, 2000; Schoof and Hindmarsh, 2010; Docquier et al., 2011; Schoof, 2011) unless the ice is moving rapidly on the ground with low basal friction~~and~~ , when the SSA equations are accurate both upstream and downstream of the GL. ~~The solution to the linearized FS equations close to the GL is investigated using perturbation theory in (Schoof, 2011)~~ ~~.~~

The evolution of the GL in simulations is sensitive to the ~~ice model ,~~ model equations and the basal friction ~~model, and numerical parameters~~law. In a major effort MISMIP ~~(Pattyn et al., 2013, 2012)~~(Pattyn et al., 2012, 2013), different ice models and implementations solve the same ice flow problems and the predicted GL steady state and transient GL motion are compared. The results ~~depend~~ show that the position of the GL depends on the model equations ~~and the mesh resolution~~ (Pattyn et al., 2013). The prediction of the GL and the SLR is different for different ice ~~equations~~ models such as FS and SSA ~~also in~~ (Pattyn and Durand, 2013). Including equations with vertical shear stress at the GL such as the FS equations seems to be crucial.

~~The flotation condition determines where the GL is in SSA in (Docquier et al., 2011; Drouet et al., 2013). It is based on Archimedes' principle for an ice column immersed in water. The~~

The friction laws at the ice base depend on the effective pressure, the basal velocity, and the distance to the GL in different combinations in ~~(Brondex et al., 2017; Gagliardini et al., 2015; Gladstone et al., 2017; Leguy et al., 2014)~~Leguy et al. (2014); Gagliardini . The GL position and the SLR vary considerably depending on the choice of friction ~~model~~law. Given the friction ~~model~~law, the results are sensitive to its model parameters too (Gong et al., 2017).

1.3 Numerical methods

Parameters in the numerical methods also influence the GL migration. It is observed in ~~(Durand et al., 2009b)~~ Durand et al. (2009b) that the mesh resolution along the ice bed has to be fine to obtain reliable solutions with FS in GL simulations. The GL is then located in a node of the fixed or static mesh. A mesh size below 1 km is necessary in ~~(Larour et al., 2019)~~ Larour et al. (2019) to resolve the features at the GL. Adaptive meshes for a finite volume discretization of an approximation of the FS equations are employed in ~~(Cornford et al., 2013)~~ Cornford et al. (2013) to study the GL retreat and loss of ice in West Antarctica. The FS solutions of benchmark problems in ~~(Pattyn et al., 2013)~~ Pattyn et al. (2013) computed by an implementation of the finite element method (FEM) in Elmer/ICE (Gagliardini et al., 2013) and FELIX-S (Leng et al., 2012) are compared in

~~(Zhang et al., 2017)~~Zhang et al. (2017). The differences between the codes are attributed to different treatment of a friction parameter at the GL and different assignment of grounded and floating nodes and element faces.

A subgrid scheme introduces an inner structure in the discretization element or mesh volume where the GL is located. Such ~~a~~ schemes have been developed for simplifications of the FS equations. A subgrid model for the GL is tested in ~~(Gladstone et al., 2010b) for the~~ Gladstone et al. (2010b) for the one dimensional (1D) SSA equation where the flotation condition for the ice defines the position of the GL. The GL migration is determined by the two dimensional (2D) SSA equations discretized by the finite element method (FEM) in ~~(Seroussi et al., 2014)~~Seroussi et al. (2014). Subgrid models at the GL are compared to a model without an internal structure in the element. The conclusion is that sub-element parameterization is necessary. A shallow approximation to FS with a subgrid scheme on coarse meshes is compared to FS in ~~(Feldmann et al., 2014)~~ Feldmann et al. (2014) with similar results for the GL migration. Subgrid modeling and adaptivity are compared in ~~(Cornford et al., 2016)~~ Cornford et al. (2016) for a vertically integrated model. The thickness of the ice above flotation determines if the ice is grounded or floating. A fine mesh resolution is necessary for converged GL positions with FS in ~~(Durand et al., 2009a, b). The purpose of a subgrid scheme is to avoid such fine meshes.~~ ~~The fine mesh resolution needed in GL simulations with the FS equations would require large computational efforts in 3D in long time intervals. Since the GL moves long distances in palaeo simulations, a~~ Durand et al. (2009a, b). A dynamic mesh refinement and coarsening of the mesh following the GL ~~is necessary. The alternative pursued here with FEM~~ would solve the problem in palaeo simulations when the GL moves long distances. An alternative is to introduce a subgrid scheme in the mesh elements where the GL is located in a static mesh and keep the mesh size coarser.

~~The subgrid scheme is~~

1.4 Our proposed method and outline of the paper

From the above we conclude that

- the prediction of SLR is very sensitive to the position of the GL and the numerical treatment in a neighbourhood of the GL,
- it seems crucial that the ice model includes equations with vertical shear stress in the neighbourhood of the GL,
- one way to avoid the fine meshes that are otherwise needed close to the GL, is to introduce a subgrid scheme in the discretization element where the GL is located.

For this purpose, we develop a numerical method for the FS equations in two dimensions introducing a subgrid scheme in the mesh element where the GL is located. Since the subgrid scheme is restricted to one element in a 2D vertical ice ~~and is therefore~~ this is computationally inexpensive. In an extension to 3D, the subgrid scheme would be applied along a line of elements in 3D. The results with numerical modeling will always depend on the mesh resolution but can be more or less sensitive to the mesh spacing and time steps. ~~Our subgrid scheme is aiming at improving the accuracy in GL simulations for a static mesh.~~We solve the FS equations in a 2D vertical ice with the Galerkin method implemented in Elmer/ICE (Gagliardini et al., 2013). A subgrid discretization is proposed and tested for the element where the GL is located. The boundary conditions are imposed by Nitsche's method at the ice base in the weak formulation of the equations ~~(Nitsche, 1971; Reusken et al., 2017; Urquiza et al., 2014)~~ (Nitsche, 1971; Urquiza et al., 2014; Reusken et al., 2017). The linear Stokes equations are solved in ~~(Chouly et al., 2017a)~~ Chouly et al. (2017a) with Nitsche's treatment of the boundary conditions. They solve the equations for the displacement but here we solve for the velocity using similar numerical techniques to weakly impose the Dirichlet boundary conditions on the normal velocity at the base. The frictional force in the tangential direction is applied on part of the element with the GL. The position of the GL within the element is determined in agreement with theory developed for the linearized FS in ~~(Schoof, 2011)~~ Schoof (2011).

The paper is organized as follows. Section 2 is devoted to the presentation of the mathematical model of the ice sheet dynamics. In Sect. 3, the numerical discretization with FEM is given while the subgrid scheme around the GL is found in Sect. 4. The numerical results for a MISMIP problem are presented in Sect. 5. The extension to three dimensions (3D) is discussed in Sect. 6 and finally some conclusions are drawn in Sect. 7.

2 Ice model

2.1 The full Stokes (FS) equations

We use the FS equations in a 2D vertical ice with coordinates $\mathbf{x} = (x, z)^T$ for modeling ~~of~~ the flow of an ice sheet (Hutter, 1983). ~~These~~ The nonlinear partial differential equations (PDEs) in the interior of the ice domain Ω are given by

$$\begin{cases} \nabla \cdot \mathbf{u} = 0, \\ -\nabla \cdot \sigma = \rho \mathbf{g}, \end{cases} \tag{1}$$

where the stress tensor is $\sigma = \tau(\mathbf{u}) - p\mathbb{I}$ and the deviatoric stress tensor is $\tau(\mathbf{u}) = 2\eta(\mathbf{u})\dot{\epsilon}(\mathbf{u})$. The strain rate tensor is defined by

$$\dot{\epsilon}(\mathbf{u}) = \frac{1}{2}(\nabla \mathbf{u} + \nabla \mathbf{u}^T) = \begin{pmatrix} \dot{\epsilon}_{11} & \dot{\epsilon}_{12} \\ \dot{\epsilon}_{12} & \dot{\epsilon}_{22} \end{pmatrix}, \tag{2}$$

$\mathbb{I}$ is the identity matrix, and the viscosity is defined by Glen's flow law

$$\eta(\mathbf{u}) = \frac{1}{2} \left(\mathcal{A}(T')\right)^{-\frac{1}{n}} \dot{\epsilon}_e^{\frac{1-n}{n}}, \qquad \dot{\epsilon}_e = \sqrt{\frac{1}{2}\mathrm{tr}(\dot{\epsilon}(\mathbf{u})\dot{\epsilon}(\mathbf{u}))}. \tag{3}$$

Here $\mathbf{u} = (u, w)^T$ is the vector of velocities, ρ is the density of the ice, p denotes the pressure, and the gravitational ~~acceleration in the z-direction~~ vector is denoted by $\mathbf{g}$. The viscosity η is a function of the rate factor $\mathcal{A}(T')$ ~~describes how the viscosity depends on the pressure melting point corrected temperature T'.~~ where T' is the ice temperature. For isothermal flow assumed here, the rate factor $\mathcal{A}$ is constant. Finally, n is usually taken to be 3.

2.2 Boundary conditions

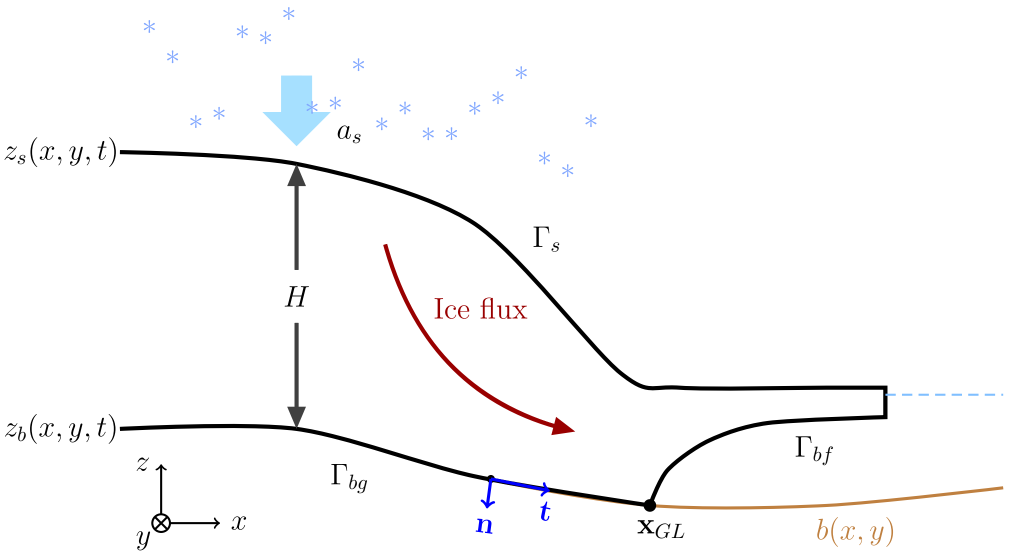

Figure 1. A two dimensional schematic view of a marine ice sheet.

At the boundary Γ of the ice domain Ω we define the normal outgoing vector $\mathbf{n}$ and tangential vector $\mathbf{t}$ ~~,~~ (see Fig. 1). In the 2D vertical case considered here, the ice sheet geometry is constant in y. The ice surface is denoted by Γ_s and the ice base is $\Gamma_b = \Gamma_{bg} \cup \Gamma_{bf}$. At Γ_s and Γ_{bf}, the floating part of Γ_b, we have that

$$\sigma\mathbf{n} = \mathbf{f}_s \quad , \quad \sigma\mathbf{n} = \mathbf{f}_{bf}, \tag{4}$$

respectively. The ice is stress-free at Γ_s, $\mathbf{f}_s = 0$, and $\mathbf{f}_{bf} = -p_w\mathbf{n}$ at the ice/ocean interface Γ_{bf} where p_w is the water pressure. Let

$$\sigma_{\mathbf{nt}} = \mathbf{t}\cdot\sigma\mathbf{n},\ \sigma_{\mathbf{nn}} = \mathbf{n}\cdot\sigma\mathbf{n},\ u_{\mathbf{t}} = \mathbf{t}\cdot\mathbf{u},$$

where $\boldsymbol{\sigma}_{\mathbf{nn}}$ and $\boldsymbol{\sigma}_{\mathbf{nt}}$ are the normal and tangential components of the stress and $u_{\mathbf{t}}$ is the tangential component of the ice velocity at the ice base. Then for the slip boundary Γ_{bg}, the grounded part of Γ_b where the ice ~~is~~ rests on the bedrock, we have a friction law for the sliding ice

$$\sigma_{\mathbf{nt}} + \beta(\mathbf{u}, \mathbf{x})u_{\mathbf{t}} = 0, \quad u_{\mathbf{n}} = \mathbf{n}\cdot\mathbf{u} = 0, \quad -\sigma_{\mathbf{nn}} \geq p_w, \tag{5}$$

where $u_{\mathbf{n}}$ is the normal component of the ice velocity. The type of friction law is determined by the friction coefficient β (≥ 0). At Γ_{bf}, there is a balance between $\sigma_{\mathbf{nn}}$ and p_w and the contact is friction-free, $\beta = 0$~~, then~~. Then

$$\sigma_{\mathbf{nt}} = 0, \qquad -\sigma_{\mathbf{nn}} = p_w. \tag{6}$$

At the GL, the boundary condition switches from $\beta > 0$ and $u_{\mathbf{n}} = 0$ on Γ_{bg} to $\beta = 0$ and a free $u_{\mathbf{n}}$ on Γ_{bf}. In a 2D vertical ice, the GL is the point (x_{GL}, z_{GL}) shared between Γ_{bg} and Γ_{bf}.

The ocean surface is at $z = 0$, and $p_w = -\rho_w g z_b$~~where ρ_w is the~~. The density of sea water is denoted by ρ_w, z_b is the z-coordinate of Γ_b, and g is the vertical component of the gravitational ~~acceleration~~force.

2.3 The free surface equations

The boundaries Γ_s and Γ_b are time-dependent and move according to two free surface equations. The boundary Γ_{bg} follows the fixed bedrock with coordinates $(x, b(x))$.

The z-coordinate of the ice surface position $z_s(x,t)$ at Γ_s (see Fig. 1) is the solution of an advection equation

$$\frac{\partial z_s}{\partial t} + u_s \frac{\partial z_s}{\partial x} - w_s = a_s, \tag{7}$$

where a_s denotes the surface mass balance and $\mathbf{u}_s = (u_s, w_s)^T$ the velocity at the ice surface in contact with the atmosphere. Similarly, the z-coordinate for the ice base z_b of the floating ice at Γ_{bf} satisfies

$$\frac{\partial z_b}{\partial t} + u_b \frac{\partial z_b}{\partial x} - w_b = a_b, \tag{8}$$

where a_b is the basal mass balance and $\mathbf{u}_b = (u_b, w_b)^T$ the velocity of the ice at Γ_{bf}. On Γ_{bg}, $z_b = b(x)$ and on Γ_{bf}, ~~$z_b < 0$~~$z_b > b(x)$.

The thickness of the ice is denoted by $H = z_s - z_b$ and depends on x and t.

2.4 ~~The~~ A first order solution close to the grounding line

The 2D vertical solution of the FS equations in Eq. (1) with a constant viscosity, $n = 1$ in Eq. (3), is expanded in small parameters in ~~(Schoof, 2011)~~Schoof (2011). The solutions in different regions around the GL are connected by matched asymptotics. Upstream of the GL at the grounded part, $x < x_{GL}$, the leading terms in the expansion satisfy a simple relation in scaled variables close to the GL. Across the GL, the ice velocity u, the flux of ice uH, and the depth integrated normal or longitudinal stress τ_{11} in Eq. (2) are continuous. By including higher order terms in the expansion in small parameters, it is shown in Schoof (2011, Sect. 4.7) that the ice surface slope is continuous and Archimedes' flotation condition

$$H\rho = -z_b \rho_w \tag{9}$$

is not satisfied immediately downstream of the GL. A rapid variation in the vertical velocity w in a short distance interval at the GL causes oscillations in the ice surface in the analysis as ~~observed also~~ also observed in FS simulations in ~~(Durand et al., 2009a).~~ Durand et al. (2009a). The flotation condition in (9) determines where the GL is in SSA in Docquier et al. (2011); D .In ~~(Schoof, 2011, Ch. 4.3)~~Schoof (2011, Sect. 4.3), the solution to the FS in a 2D vertical ice is expanded in two parameters, ν and ϵ. The aspect ratio of the ice ν is the quotient between a typical scale of the thickness of the ice $\mathcal{H}$ and a horizontal length scale $\mathcal{L}$, $\nu = \mathcal{H}/\mathcal{L}$, and ϵ is ν times the quotient between the longitudinal and the shear stresses τ_{11} and τ_{12} in Eq. (2). If $\nu^{5/2} \ll \epsilon \ll 1$ then in a boundary layer close to the GL and $x < x_{GL}$ it follows from the equations that the leading terms in the solution in scaled variables satisfy

$$\tau_{22} - p = \sigma_{22} = \rho g(z - z_s). \tag{10}$$

On floating ice $\tau_{22} - p + p_w = 0$ and the hydrostatic flotation criterion Eq. (9) is fulfilled. This is a first order approximation of the second relation in Eq. (6). On the grounded ice domain, we have $\tau_{22} - p + p_w < 0$.

Introducing the notation

$$\chi_a(x,z) = \tau_{22} - p + p_w = \rho g(z - z_s(x)) - \rho_w g z_b(x), \tag{11}$$

and letting $H_{bw} = -z_b$ be the thickness of the ice below the sea level yields

$$\chi_a(x,z_b) = -g(\rho H - \rho_w H_{bw}). \tag{12}$$

If $x < x_{GL}$ then $\chi_a < 0$ in the neighborhood of x_{GL} on Γ_{bg} and if $x > x_{GL}$ then $\chi_a = 0$ and Eq. (9) holds true on Γ_{bf}. Suppose that z_s and z_b are linear in x. Then χ_a is also linear in x. In numerical experiments with the linear FS $(n = 1)$ in ~~(Nowicki and Wingham, 2008)~~Nowicki and Wingham (2008), $\chi_a(x,z_b)$ ~~in the original variables~~ varies linearly in x for $x < x_{GL}$.

In Sect. 4, ~~$\chi_a(x,z_b)$ is an approximation of the expression used~~ we mimic the same idea but use an indicator $\chi(x)$ or $\tilde{\chi}(x)$ derived from the solutions of the nonlinear FS equations to estimate the GL position. These indicators are approximated by $\chi_a(x,z_b)$.

3 Discretization by FEM

In this section we state the weak form of Eq. (1) and introduce the spatial FEM discretization used for Eq. (1) and give the time-discretization of Eq. (7) and (8).

3.1 The weak form of the FS equations

We start by defining the mixed weak form of the FS equations. Introduce $k = 1 + 1/n$, $k^* = 1 + n$ with n from Glen's flow law and the spaces

$$\boldsymbol{V}_k = \{\mathbf{v} : \mathbf{v} \in (W^{1,k}(\Omega))^2\}, \quad Q_{k^*} = \{q : q \in L^{k^*}(\Omega)\}, \tag{13}$$

see, e.g. ~~(Chen et al., 2013; Jouvet and Rappaz, 2011; Martin and Monnier, 2014)~~Jouvet and Rappaz (2011, Eq. (3.7)), Chen et al. (2013, S , Martin and Monnier (2014, Eq. (21)). The weak solution $(\mathbf{u},p)$ of Eq. (1) is obtained as follows. Find $(\mathbf{u},p) \in \boldsymbol{V}_k \times Q_{k^*}$ such that for all $(\mathbf{v},q) \in \boldsymbol{V}_k \times Q_{k^*}$ the equation

$$A((\mathbf{u},p),(\mathbf{v},q)) + B_\Gamma(\mathbf{u},\mathbf{v},p) + B_\mathcal{N}(\mathbf{u},\mathbf{v},q) = F(\mathbf{v}) + F_\Gamma(\mathbf{v}), \tag{14}$$

is satisfied, where

$$A((\mathbf{u},p),(\mathbf{v},q)) = \int\limits_{\Omega} 2\eta(\mathbf{u})\dot{\epsilon}(\mathbf{u}) : \dot{\epsilon}(\mathbf{v}) \;\,\mathrm{d}\mathbf{x} - b(\mathbf{u},q) - b(\mathbf{v},p),$$

$$b(\mathbf{u},q) = \int\limits_{\Omega} q\nabla\cdot\mathbf{u} \;\,\mathrm{d}\mathbf{x},$$

$$B_{\Gamma}(\mathbf{u},\mathbf{v},p) = -\int\limits_{\Gamma_{bg}} (\sigma_{\mathbf{nn}}(\mathbf{u},p)\mathbf{n}\cdot\mathbf{v} + \sigma_{\mathbf{nt}}(\mathbf{u},p)\mathbf{t}\cdot\mathbf{v}) \;\,\mathrm{d}s = \int\limits_{\Gamma_{bg}} (-\sigma_{\mathbf{nn}}(\mathbf{u},p)\mathbf{n}\cdot\mathbf{v} + \beta(\mathbf{t}\cdot\mathbf{u})(\mathbf{t}\cdot\mathbf{v})) \;\,\mathrm{d}s,$$

$$B_{\mathcal{N}}(\mathbf{u},\mathbf{v},q) = -\int\limits_{\Gamma_{bg}} \sigma_{\mathbf{nn}}(\mathbf{v},q)\mathbf{n}\cdot\mathbf{u}\,\mathrm{d}s + \gamma_0 \int\limits_{\Gamma_{bg}} \frac{1}{h}(\mathbf{n}\cdot\mathbf{u})(\mathbf{n}\cdot\mathbf{v})\,\mathrm{d}s,$$

$$F(\mathbf{v}) = \int\limits_{\Omega} \rho\mathbf{g}\cdot\mathbf{v} \;\,\mathrm{d}\mathbf{x},$$

$$F_{\Gamma}(\mathbf{v}) = -\int\limits_{\Gamma_{bf}} p_w\mathbf{n}\cdot\mathbf{v} \;\,\mathrm{d}s$$

The last term in $B_{\mathcal{N}}$ is added in the weak form in Nitsche's method (Nitsche, 1971) to impose the Dirichlet condition $u_{\mathbf{n}} = 0$ weakly on Γ_{bg}. It can be considered as a penalty term. ~~The value~~ Since $\mathbf{u} = u_{\mathbf{n}}\mathbf{n} + u_{\mathbf{t}}\mathbf{t}$, the contribution of the tangential force can also be written $\beta\mathbf{u}\cdot\mathbf{v}$ when $u_{\mathbf{n}} = 0$. The value of the positive parameter γ_0 depends on the ~~physical problem~~ physical problem and h is a measure of the mesh size on Γ_b. The sensitivity of the GL positions for different values of γ_0 is shown in Sect. 5. The first term in $B_{\mathcal{N}}$ symmetrizes the boundary term $B_{\Gamma} + B_{\mathcal{N}}$ on Γ_{bg} and vanishes when $u_{\mathbf{n}} = 0$. The boundary term $F_{\Gamma}(\mathbf{v})$ is from the buoyancy force at the ice/ocean interface in (6) where p_w depends on z_b on Γ_{bf}.

3.2 The discretized FS equations

We employ linear Lagrange elements with Galerkin Least Square (GLS) stabilization (Franca and Frey, 1992; Helanow and Ahlkrona, 2018) to avoid spurious oscillations in the pressure using the standard setting in Elmer/ICE (Gagliardini et al., 2013) approximating solutions in the spaces $\boldsymbol{V}_k$ and Q_{k^*} in Eq. (13).

The mesh is constructed from a footprint mesh on the ice base and then extruded with the same number of layers equidistantly in the vertical direction according to the thickness of the ice sheet. To simplify the implementation in 2D, the footprint mesh on the ice base consists of $N+1$ nodes at $\mathbf{x}_i = (x_i, z_b(x_i))$, $i = 0, \ldots, N$, with x-coordinates x_i and a constant mesh size $\Delta x = x_i - x_{i-1}$.

In general, the GL is somewhere in the interior of an interval $[x_{i-1}, x_i]$ and it crosses the interval boundaries as it moves forward in the advance phase and backward in the retreat phase of the ice. The advantage with Nitsche's way of formulating the boundary conditions is that if $x_{GL} \in [x_{i-1}, x_i]$ then the boundary integral over the interval can be split into two parts in Eq. (14) such that $(x, z_b(x)) \in \Gamma_{bg}$ when $x \in [x_{i-1}, x_{GL}]$ and if $x \in [x_{GL}, x_i]$ then $(x, z_b(x)) \in \Gamma_{bf}$ ~~as follows~~. In the GL element, we have

$$B_\Gamma + B_\mathcal{N} = \int\limits_{[x_{i-1},x_{GL}]} -(\sigma_{\mathbf{nn}}(\mathbf{u},p)\mathbf{n}\cdot\mathbf{v} + \sigma_{\mathbf{nn}}(\mathbf{v},q)\mathbf{n}\cdot\mathbf{u}) + \beta(\mathbf{t}\cdot\mathbf{u})(\mathbf{t}\cdot\mathbf{v}) + \frac{\gamma_0}{h}(\mathbf{n}\cdot\mathbf{u})(\mathbf{n}\cdot\mathbf{v})\ \mathrm{d}s,$$

$$F_\Gamma = -\int\limits_{[x_{GL},x_i]} p_w \mathbf{n}\cdot\mathbf{v}\ \mathrm{d}s, \tag{15}$$

with the integration element $\mathrm{d}s$ following Γ_b. There is a change of the boundary condition in the middle of the FEM element where the GL is located. With a strong formulation of the boundary condition $u_\mathbf{n} = 0$, the basis functions in $\boldsymbol{V}_k$ share this property and the condition changes from the grounded node x_{i-1} where the basis function satisfies $u_\mathbf{n} = 0$ ~~and~~ to the floating node at x_i with a free $u_\mathbf{n}$ without taking the position of the GL inside $[x_{i-1}, x_i]$ into account. With the weak formulation in Nitsche's method~~no basis function satisfies~~ , the standard basis functions we use do not satisfy $u_\mathbf{n} = 0$ strictly~~but the~~ . The boundary condition is imposed on the solution by the additional penalty term in (14) and this term may change inside an element as in (15).

The resulting system of nonlinear equations form a nonlinear complementarity problem (Christensen et al., 1998). The distance d between the base of the ice and the bedrock at time t and at x is ~~$d(x,t) = z_b(x,t) - b(x) \geq 0.$~~

$$d(x,t) = z_b(x,t) - b(x) \geq 0. \tag{16}$$

If $d > 0$ on Γ_{bf} then the ice is not in contact with the bedrock and $\sigma_{\mathbf{nn}} + p_w = 0$ and if $\sigma_{\mathbf{nn}} + p_w < 0$ on Γ_{bg} then the ice and the bedrock are in contact and $d = 0$. Hence, the complementarity relation in the vertical direction is

$$d(x,t) \geq 0,\ \sigma_{\mathbf{nn}} + p_w \leq 0, \quad d(x,t)(\sigma_{\mathbf{nn}} + p_w) = 0 \text{ on } \Gamma_b. \tag{17}$$

The contact friction law is such that $\beta > 0$ when $x < x_{GL}$ and $\beta = 0$ when $x > x_{GL}$. The complementarity relation along the ~~slope~~ ice base at x is then the non-negativity of d and

$$\beta \geq 0,\ \beta(x,t)d(z_b(x,t) - b(x)) = 0 \text{ on } \Gamma_b. \tag{18}$$

In particular, these relations are valid at the nodes $x = x_j$, $j = 0, 1, \ldots, N$.

The complementarity condition also holds for $u_\mathbf{n}$ and $\sigma_{\mathbf{nn}}$ such that

$$\sigma_{\mathbf{nn}} + p_w \leq 0, \quad u_\mathbf{n}(\sigma_{\mathbf{nn}} + p_w) = 0 \text{ on } \Gamma_b, \tag{19}$$

without any sign constraint on $u_\mathbf{n}$ except for the retreat phase when the ice leaves the ground and $u_\mathbf{n} < 0$.

Similar implementations for contact problems using Nitsche's method are found in ~~(Chouly et al., 2017a, b)~~Chouly et al. (2017a, b) , where the unknowns in the PDEs are the displacement fields instead of the velocity in Eq. (1). Analysis in ~~(Chouly et al., 2017a)~~ Chouly et al. (2017a) suggests that Nitsche's method for the contact problem can provide a stable numerical solution with an optimal convergence rate.

The nonlinear equations, Eq. (14), for the nodal values of $\mathbf{u}$ and p are solved by Picard iterations. The system of linear equations in every Picard iteration is solved directly by using the MUMPS linear solver in Elmer/ICE. The condition on

$d_j = d(x_j)$ is used to decide if the node x_j is geometrically grounded or floating. It is computed at each ~~timestep and~~ time step and is not changed during the nonlinear iterations (Picard). The procedure for solution of the nonlinear FS equations is outlined in Algorithm 1. In two dimensions, the GL will be located in one element.

Algorithm 1 Solve the FS equations

For a given mesh, compute $d_j, j = 0, 1, ..., N$, for all the nodes x_j at the ice base.
Mark node j as geometrically grounded if $d_j < 10^{-3}$, otherwise floating.
Find the element which contains both geometrically grounded and floating nodes, and mark the grounded node in this element as 'GL node'.
Compute the residual of the FS equations with the initial guess of the solution.
while the residual is larger than the tolerance **do**
  Assemble the FEM matrix for the interior of the domain Ω.
  for the boundary elements on Γ_b **do**
    if has 'GL ~~nodes~~node' **then**
      Mark the current element as a 'potential GL element'.
      Use the subgrid scheme in Algorithm 3 of Sect. 4 for the assembly.
    else
      Assemble the boundary element.
    end if
  end for
  Solve the linearized FS equations for a correction of the solution.
  Compute the solution and the residual.
end while

3.3 Discretization of the advection equations

The advection equations for the moving ice boundary in Eq. (7) and (8) are discretized in time by a finite difference method and in space by FEM with linear Lagrange elements for z_s and z_b. An artificial diffusion stabilization term is added, making the spatial discretization behave like an upwind scheme in the direction of the velocity as implemented in Elmer/ICE.

The advection equations Eq. (7) and Eq. (8) are integrated in time by a semi-implicit method of first order accuracy. Let $c = s$ or b. Then the solution is advanced from time ~~t^n to $t^{n+1} = t^n + \Delta t$ with the timestep~~ t^ℓ to $t^{\ell+1} = t^\ell + \Delta t$ with the time step Δt by

$$z_c{}^{\cancel{n+1}\,\ell+1} = z_c{}^{\cancel{n}\,\ell} + \Delta t(a_c{}^{\cancel{n}\,\ell} - u_c{}^{\cancel{n}\,\ell}\cancel{\frac{\partial z_c^{n+1}}{\partial x}}\frac{\partial z_c^{\ell+1}}{\partial x} + w_c{}^{\cancel{n}\,\ell}). \tag{20}$$

The spatial derivative of z_c is approximated by FEM as described above. A system of linear equations is solved at ~~t^{n+1} for z_c^{n+1}~~ $t^{\ell+1}$ for $z_c^{\ell+1}$. This time discretization and its properties are discussed in ~~(Cheng et al., 2017) and summarized as~~ Cheng et al. (2017) and summarized in Algorithm 2.

Algorithm 2 Time scheme of the GL migration problem

Start from an initial geometry Ω^0 defined by z_b^0, z_s^0.
for $\ell = 0$ to $T/\Delta t - 1$ **do**
  Solve the FS equations on Ω^ℓ with Algorithm 1, to get the solution $\mathbf{u}^\ell$.
  Solve for $z_b^{\ell+1}$ and $z_s^{\ell+1}$ with $\mathbf{u}^\ell$ by the semi-implicit Euler method.
  Use $z_b^{\ell+1}$ and $z_s^{\ell+1}$ to update $\Omega^{\ell+1}$.
end for

A numerical stability problem in z_b is encountered in the boundary condition at Γ_{bf} when the FS equations are solved in ~~(Durand et al., 2009a)~~Durand et al. (2009a). It is resolved by expressing z_b in p_w at Γ_{bf} with a damping term. An alternative interpretation of the idea in ~~(Durand et al., 2009a)~~ Durand et al. (2009a) and an explanation follow below.

The relation between $u_{\mathbf{n}}$ and $u_{\mathbf{t}}$ at Γ_{bf} and $\mathbf{u}_b = \mathbf{u}(x, z_b(x))$ is

$$\mathbf{u}_b = \begin{pmatrix} u_b \\ w_b \end{pmatrix} = \begin{pmatrix} z_{bx} \\ -1 \end{pmatrix} \frac{u_{\mathbf{n}}}{\sqrt{1+z_{bx}^2}} + \begin{pmatrix} 1 \\ z_{bx} \end{pmatrix} \frac{u_{\mathbf{t}}}{\sqrt{1+z_{bx}^2}}, \tag{21}$$

where z_{bx} denotes $\partial z_b/\partial x$. Inserting u_b and w_b from Eq. (21) into Eq. (8) yields

$$\frac{\partial z_b}{\partial t} = a_b - u_{\mathbf{n}}\sqrt{1+z_{bx}^2}\cancel{,}. \tag{22}$$

Instead of discretizing Eq. (22) explicitly at ~~t^{n+1} with $u_{\mathbf{n}}^n$ to determine p_w^{n+1}~~$t^{\ell+1}$ with $u_{\mathbf{n}}^\ell$ to determine $p_w^{\ell+1}$, the base coordinate is updated implicitly

$$z_b^{\cancel{n+1}\ell+1} = z_b^{\cancel{n}\ell} + \Delta t\left(a_b^{\cancel{n+1}\ell+1} - u_{\mathbf{n}}^{\cancel{n+1}\sqrt{1+(z_{bx}^{n+1})^2}\,\ell+1}\sqrt{1+(z_{bx}^{\ell+1})^2}\right) \tag{23}$$

in the ~~solution of~~ evaluation of p_w in $F_\Gamma(\mathbf{v})$ in Eq. (14).

Assuming that z_{bx} is small, the ~~timestep~~time step restriction in Eq. (23) is estimated by considering a 2D slab of the floating ice of width Δx and thickness H. Newton's law of motion yields

$$M\dot{u}_{\mathbf{n}} = Mg - \Delta x p_w,$$

where $M = \Delta x(z_s - z_b)\rho$ is the mass of the slab. Dividing by M, integrating in time for $u_{\mathbf{n}}(t^m)$, letting ~~$m = n+1$ or n~~$m = \ell+1$ or ℓ, and approximating the integral by the trapezoidal rule for the quadrature yields

$$u_{\mathbf{n}}(t^m) = \int_0^{t^m} g + \frac{g\rho_w}{\rho}\frac{z_b}{z_s - z_b}\,\mathrm{d}s \approx gt^m + \frac{g\rho_w}{\rho}\sum_{i=0}^{m}\alpha_i \frac{z_b^i}{z_s^i - z_b^i}\Delta t = u_{\mathbf{n}}^m,$$

with the parameters

$$\alpha_i = 0.5,\; i = 0, m, \quad \alpha_i = 1,\; i = 1, \ldots, m-1.$$

Then insert $u_{\mathbf{n}}^m$ into Eq. (23). All terms in $u_{\mathbf{n}}^m$ from ~~timesteps~~ time steps $i < m$ are collected in the sum $\Delta t F^{m-1}$. Then Eq. (23) can be written

$$z_b{}^{\cancel{n+1}\ell+1} = z_b{}^{\cancel{n}\ell} - \Delta t^2 \frac{g\rho_w}{2\rho} \frac{z_b^m}{z_s^m - z_b^m} + \Delta t \left(a_b{}^{\cancel{n}\ell} - g t^m - \Delta t F^{m-1} \right). \tag{24}$$

For small changes in z_b in Eq. (24), the explicit method with $\cancel{m = n}$ $m = \ell$ is stable when Δt is so small that

$$|1 - \Delta t^2 \frac{g\rho_w}{2H\rho}| \le 1. \tag{25}$$

When $H = 100$ m on the ice shelf, $\Delta t < 6.1$ s which is far smaller than the stable steps for Eq. (20). Choosing the implicit scheme with $\cancel{m = n+1}$ $m = \ell + 1$, the bound on Δt is

$$1/|1 + \Delta t^2 \frac{g\rho_w}{2H\rho}| \le 1, \tag{26}$$

i.e. there is no bound on positive Δt for stability but accuracy will restrict Δt.

Much longer stable ~~timesteps~~ time steps are possible at the surface and the base of the ice with a semi-implicit method Eq. (20) and a fully implicit method Eq. (23) compared to an explicit method. For example, the ~~timestep~~ time step for the problem in Eq. (20) with 1 km mesh size can be up to a couple of months. Therefore, we use the scheme in Eq. (20) for Eqs. (7) and (8) and the scheme in Eq. (23) for Eq. (22) and p_w as in ~~(Durand et al., 2009a)~~ Durand et al. (2009a). The difference between the approximations of z_b in Eq. (20) and (23) is of $\mathcal{O}(\Delta t^2)$.

4 Subgrid scheme around the grounding line

The basic idea of the subgrid scheme for the FS equations in this paper follows the GL parameterization (SEP3) for SSA in ~~(Seroussi et al., 2014)~~ Seroussi et al. (2014) and the analysis for FS in ~~(Schoof, 2011)~~ Schoof (2011). The GL is located at the position where the ice is on the ground and the flotation criterion is perfectly satisfied such that $\sigma_{\mathbf{nn}} = -p_w$. In the FS equations, the hydrostatic assumption Eq. (9) may not be valid close to the GL. Therefore, the GL position can not be determined by simply checking the total thickness of the ice H against the depth below sea level H_{bw}. Instead, the flotation criterion is computed by comparing the water pressure with the numerical normal stress component orthogonal to the boundary ~~, as suggested~~ inspired by the first order analysis in Sect. 2.4.

~~The indicator is here defined by~~

$$\cancel{\chi(\mathbf{x}) = \sigma_{\mathbf{nn}} + p_w,}$$

~~which vanishes on the floating ice and is negative and approximately equal to~~ $\cancel{\chi_a = \tau_{22} - p + p_w}$ ~~in on the ground since the slope of the bedrock is small and~~ $\cancel{\mathbf{n} \approx (0, -1)^T}$~~.~~

The numerical solutions, e.g. ~~(Gagliardini et al., 2016; Gladstone et al., 2017)~~ Gagliardini et al. (2016); Gladstone et al. (2017), converge to the analytical solution of the FS PDE as the mesh size decreases. The analytical solution satisfies $z_b(x,t) > b(x)$ with the boundary conditions in Eq. (6) at the base of the floating ice, and where the ice is in contact with the bedrock

$z_b(x,t) = b(x)$, the boundary conditions are given by Eq. (5). Examples of the analytical solution are demonstrated by the thin light blue lines in ~~Fig~~Figs. 2 and 3 with a black '$*$' at the analytical GL position $\mathbf{x}_{GL}$. The two figures share the same analytical solution. However, as illustrated in ~~Fig~~Figs. 2 and 3, the basal boundary of the ice $z_b(x,t)$ does not conform with the mesh from the spatial discretization. In particular, the GL position $\mathbf{x}_{GL}$ of the analytical solution does not coincide with any of the nodes, but it usually stays on the bedrock $b(x)$ between the last grounded ($\mathbf{x}_{i-1}$) and the first floating ($\mathbf{x}_i$) nodes, see ~~Fig~~Figs. 2 and 3. The linear element ~~between~~ boundary between any $\mathbf{x}_{j-1}$ and $\mathbf{x}_j$ is denoted by $\mathcal{E}_j$. The sequence of $\mathcal{E}_j, j = 1,\ldots,N$, approximates Γ_b. The grounding line element containing the GL is $\mathcal{E}_i$.

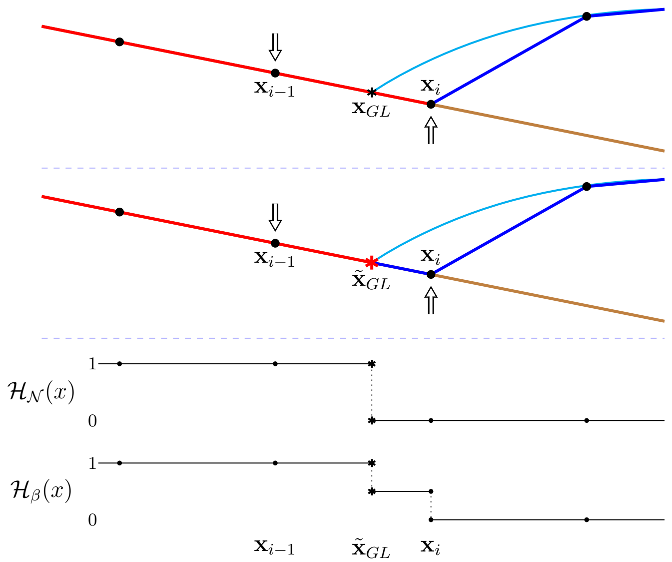

Figure 2. Schematic figure of the GL in case i, with the arrows indicating the direction of the net forces in the vertical direction. Upper panel: The last grounded and first floating nodes as defined in Elmer/ICE. The light blue line is the analytical solution of the ice sheet with the analytical GL position $\mathbf{x}_{GL}$. Middle panel: Linear interpolation to approximate the numerical GL position $\tilde{\mathbf{x}}_{GL}$. Lower panel: The step functions $\mathcal{H}_{\mathcal{N}}(x)$ and $\mathcal{H}_{\beta}(x)$ ~~which~~ indicate the area for Nitsche's penalty and slip boundary conditions.

Depending on how the mesh is created from the initial geometry and updated during the simulation, the first floating node at $\mathbf{x}_i$, as well as the GL element, can be either on the bedrock (as in Fig. 2) or at the ~~basal surface of the ice~~ ice base above the bedrock (as in Fig. 3), even though the corresponding analytical solutions are identical. Denote the situation in Fig. 2 ~~by~~ as case i, and the one in Fig. 3 ~~by~~ as case ii. The physical boundary conditions of the two cases are different only at the GL element. More precisely, in case i, the net force in the vertical direction on the node $\mathbf{x}_i$ is pointing inward, namely $\chi(\mathbf{x}_i) = \sigma_{\mathbf{nn}}(\mathbf{x}_i) + p_w(\mathbf{x}_i) > 0$, whereas in case ii, the floating condition $\sigma_{\mathbf{nn}}(\mathbf{x}_i) + p_w(\mathbf{x}_i) = 0$ is satisfied in the node $\mathbf{x}_i$. The directions of the vertical net force at the nodes $\mathbf{x}_{i-1}$ and $\mathbf{x}_i$ are shown by the arrows in the upper panels of Fig. 2 and 3. Consequently, the external forces and boundary conditions imposed on the GL element are different in the two cases. For instance, in case i, the GL element is considered as geometrically grounded (defined as in Algorithm 1), shown with red color

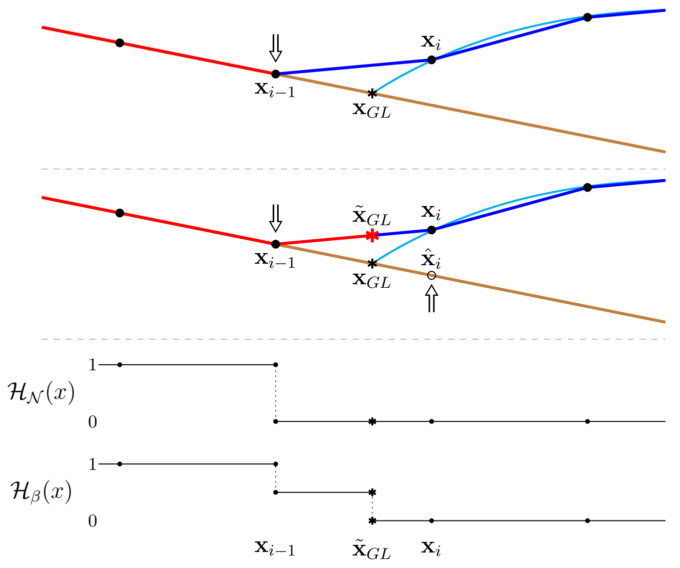

Figure 3. Schematic figure of the GL in case ii, with the arrows indicating the direction of the net ~~force~~forces in the vertical direction. Upper panel: The last grounded and first floating nodes as defined in Elmer/ICE. The light blue line is the analytical solution of the ice sheet with the analytical GL position $\mathbf{x}_{GL}$. The node $\mathbf{x}_i$ is fully geometrically floating and the net force is 0. Middle panel: Linear interpolation to approximate the numerical GL position $\tilde{\mathbf{x}}_{GL}$. The point $\hat{\mathbf{x}}_i$ on the bedrock has the same x coordinate as $\mathbf{x}_i$. Lower panel: The step functions $\mathcal{H}_{\mathcal{N}}(x)$ and $\mathcal{H}_{\beta}(x)$ ~~which~~ indicate the area for Nitsche's penalty and slip boundary conditions.

in the upper panel of Fig. 2. In case ii, the GL element is treated as geometrically floating and colored in blue in the upper panel of Fig. 3.

These two cases are similar to the LG and FF cases in ~~(Gagliardini et al., 2016)~~ Gagliardini et al. (2016) implying that the numerical solutions in the ~~the~~ two cases are different, especially on a coarse mesh (mesh size at about 100 m or larger). Thus, we propose a subgrid scheme to reduce these differences in the spatial discretization and to capture the GL migration without using a fine mesh resolution (<100 m). The schematic drawing of the subgrid scheme for the two cases is shown in the middle panels of Fig. 2 and 3. The GL element is divided into the grounded (red) and floating (blue) parts by the estimated GL position $\tilde{\mathbf{x}}_{GL}$ on $\mathcal{E}_i$, which is the numerical approximation of the analytical GL position $\mathbf{x}_{GL}$.

The GL moves toward the ocean in the advance phase and away from the ocean in the retreat phase. First, we consider case i in the *advance phase* and define the indicator by

$$\chi(\mathbf{x}) = \sigma_{\mathbf{nn}} + p_w, \tag{27}$$

which vanishes on the floating ice and is negative and approximately equal to $\chi_a = \tau_{22} - p + p_w$ in Eq. (11) on the ground since the slope of the bedrock is small and $\mathbf{n} \approx (0, -1)^T$. Because of the poor spatial resolution of the coarse mesh, $\chi(\mathbf{x}_i)$ is positive.

To determine the position $\tilde{\mathbf{x}}_{GL}$, we solve $\chi(\tilde{\mathbf{x}}_{GL}) = \sigma_{\mathbf{nn}}(\tilde{\mathbf{x}}_{GL}) + p_w(\tilde{\mathbf{x}}_{GL}) = 0$ by linear interpolation between $\chi(\mathbf{x}_{i-1})$ and $\chi(\mathbf{x}_i)$ such that

$$\tilde{\mathbf{x}}_{GL} = \mathbf{x}_{i-1} - \frac{\chi(\mathbf{x}_{i-1})}{\chi(\mathbf{x}_{i-1}) - \chi(\mathbf{x}_i)}(\mathbf{x}_{i-1} - \mathbf{x}_i). \tag{28}$$

The water pressure $p_w(\mathbf{x})$ is a linear function of $\mathbf{x}$ on the GL element and the numerical solution of $\sigma_{\mathbf{nn}}(\mathbf{x})$ is also piecewise linear on every element with the standard Lagrange elements in Elmer/ICE (Gagliardini et al., 2013). ~~In this sense, $\tilde{\mathbf{x}}_{GL}$ is the best numerical approximation of the~~ Hence, it makes sense to approximate the analytical GL position $\mathbf{x}_{GL}$ by $\tilde{\mathbf{x}}_{GL}$ by linear interpolation in the current framework. This approach fits well with case i since the indicator $\chi(\mathbf{x})$ has opposite signs at $\mathbf{x}_{i-1}$ and $\mathbf{x}_i$, see the middle panel of Fig. 2 where $\tilde{\mathbf{x}}_{GL}$ is marked by a red '$*$'. It guarantees the existence and uniqueness of $\tilde{\mathbf{x}}_{GL}$ on the GL element.

~~However, the situation in~~ Another situation in the advance phase is case ii ~~is more complicated. In the upper panel of~~ shown in Fig. 3~~, as~~. As the elements on both sides of the node $\mathbf{x}_i$ are geometrically floating, the boundary condition imposed on $\mathbf{x}_i$ becomes $\chi(\mathbf{x}_i) = \sigma_{\mathbf{nn}}(\mathbf{x}_i) + p_w(\mathbf{x}_i) = 0$. ~~Considering that the analytical GL position $\mathbf{x}_{GL}$ always stays on the bedrock,~~ However, the implicit treatment of the ice base moves the z-coordinate of the node $\mathbf{x}_i$ towards the bedrock with $u_{\mathbf{n}} > 0$ in Eq. (23) as discussed in Sect. 3.3. The result is that p_w defined by the implicit z_b in (23) satisfies $\sigma_{\mathbf{nn}} + p_w > 0$ in (27) and $\chi(\mathbf{x}_i) > 0$.

The implicit treatment of the ice base has the consequence that only case ii occurs in the *retreat phase*. When the FS equations are solved, the implicit update of the ice base with $u_{\mathbf{n}} < 0$ in Eq. (23) implies that the last grounded node in the previous time step is leaving the bedrock when the ice is retreating and the GL moves back to the adjacent element. Case i will not appear in that situation since $z_b(x_i) > b(x_i)$. In this circumstance, $\chi(\mathbf{x}_i) = 0$ in the floating node and a correction of $\chi(\mathbf{x})$ is introduced ~~in~~ into case ii by $\tilde{\chi}$ in

$$\tilde{\chi}(\mathbf{x}) = \sigma_{\mathbf{nn}}(\mathbf{x}) + p_b(\mathbf{x})\cancel{,}. \tag{29}$$

~~where~~ Here $p_b(\mathbf{x}) = -\rho_w g b(x)$ is the water pressure on the bedrock ~~and~~ corresponding to linear extrapolation of the pressure for $x > x_{GL}$ along the element on the bedrock. Furthermore, $\tilde{\chi}(\mathbf{x}) \geq \chi(\mathbf{x})$. Notice that $p_b(\mathbf{x}_i) = p_w(\hat{\mathbf{x}}_i) > p_w(\mathbf{x}_i)$, where $\hat{\mathbf{x}}_i$ is a point on the bedrock with the same x coordinate of $\mathbf{x}_i$, as illustrated in the middle panel of Fig. 3. Both $\chi(\mathbf{x})$ in (27) and $\tilde{\chi}(\mathbf{x})$ in (29) are nonlinear in $\mathbf{x}$ but the numerical approximation of them will vary linearly in $\mathbf{x}$. A solution $\tilde{\mathbf{x}}_{GL}$ ~~can be found by taking linear interpolations~~ is found by linear interpolation of $\tilde{\chi}(\mathbf{x})$ between the nodes $\mathbf{x}_{i-1}$ and $\mathbf{x}_i$ as in Eq. (28). It follows from Eq. (28) that $\tilde{\mathbf{x}}_{GL}$ is located on the element boundary, see Figs. 2 and 3. If we compare with case i, this correction can be considered as using $\sigma_{\mathbf{nn}}(\tilde{\mathbf{x}}_{GL})$ to approximate $\sigma_{\mathbf{nn}}(\mathbf{x}_{GL})$ on a virtual element between $\mathbf{x}_{i-1}$ and $\hat{\mathbf{x}}_i$~~, since the linear interpolation of $p_b(\mathbf{x})$ still provides the analytical water pressure along the bedrock.~~. ~~Therefore, the~~ The position $\tilde{\mathbf{x}}_{GL}$ is a numerical approximation of the analytical GL position, although it is not geometrically in contact with the bedrock.

~~Moreover, this correction is not necessary when the GL is advancing since the implicit treatment of the bottom surface is equivalent to moving $\mathbf{x}_i$ towards $\hat{\mathbf{x}}_i$ with $u_{\mathbf{n}} > 0$ in Eq. as discussed in Sect. 3.3.~~ Since we have $p_b(\mathbf{x}) = p_w(\mathbf{x})$ and $\chi(\mathbf{x}) = \tilde{\chi}(\mathbf{x})$ at the GL element in case i, we can simply use $\tilde{\chi}(\mathbf{x})$ to find $\tilde{\mathbf{x}}_{GL}$ for the two cases by replacing χ in (28) by $\tilde{\chi}$.

~~Then the~~

The domains Γ_{bg} and Γ_{bf} are separated at $\tilde{\mathbf{x}}_{GL}$ as in Eq. (15) and the integrals on the GL element are calculated with a high-order integration scheme as in ~~(Seroussi et al., 2014)~~Seroussi et al. (2014). We introduce two step functions $\mathcal{H}_{\mathcal{N}}(x)$ and $\mathcal{H}_{\beta}(x)$ to include and exclude quadrature points in the integration of ~~the~~ Nitsche's term and the slip boundary condition~~.~~, respectively. They are defined for case i in Fig. 2 and for case ii in Fig. 3. To achieve a reasonable ~~resolution~~ numerical accuracy within the GL element, as suggested in ~~(Seroussi et al., 2014)~~Seroussi et al. (2014), at least tenth order Gaussian quadrature is ~~required~~used.

The penalty term in Nitsche's method restricts the motion of the element in the normal direction. It is only imposed on ~~the~~ an element which is fully geometrically on the ground in case i. On the contrary in case ii, the GL element $\mathcal{E}_i$ is not in contact with the bedrock, see Fig. 3. ~~Only the~~ The normal velocity on the element should not be forced to zero and only the floating boundary condition is then used on the GL element. ~~When the FS equations are solved, the implicit update of the basal surface with $u_{\mathbf{n}} < 0$ in Eq. implies that the last grounded node in the previous timestep is leaving the bedrock when the ice is retreating and the GL moves to the adjacent element. Case 1 will not appear in that situation with a retreating GL and as in case 2 the normal velocity on the element should not be forced to zero.~~ Nitsche's penalty term should be imposed on all the fully geometrically grounded elements and partially on the GL element in the advance phase as in case i. The step function $\mathcal{H}_{\mathcal{N}}(x)$ indicates how Nitsche's method is implemented on the ~~boundary~~ basal elements, see the lower panels of Fig. 2 and 3 for the two cases. The penalty term contributes to the integration only when $\mathcal{H}_{\mathcal{N}}(x) = 1$.

The slip coefficient β is treated similarly with the step function $\mathcal{H}_{\beta}(x)$, where $\mathcal{H}_{\beta}(x) = 1$ is on the fully geometrically grounded elements and $\mathcal{H}_{\beta}(x) = 0$ on the floating elements. ~~For a smoother~~ To further smooth the transition of β at the GL, the step function is set to be 1/2 in parts of the GL element before integrating using the high order scheme. In case i, full friction is applied at the grounded part between $\mathbf{x}_{i-1}$ and $\tilde{\mathbf{x}}_{GL}$ of the GL element since this part is also geometrically grounded in the analytical solution ~~.~~ of the FS as in Fig. 2. Then, the friction is lower in the remaining part of $\mathcal{E}_i$. For the floating part between $\tilde{\mathbf{x}}_{GL}$ and $\mathbf{x}_i$ in case ii, there is no friction and $\mathcal{H}_{\beta}(x) = 0$ and we have reduced friction between $\mathbf{x}_{i-1}$ and $\tilde{\mathbf{x}}_{GL}$, see the lower panel of Fig. 3. The boundary integral Eq. (15) on $\mathcal{E}_i$ is now rewritten with the two step functions as

$$\begin{aligned} B_\Gamma + B_{\mathcal{N}} &= \int_{\mathcal{E}_i} -\mathcal{H}_{\mathcal{N}}(\sigma_{\mathbf{nn}}(\mathbf{u},p)\mathbf{n}\cdot\mathbf{v} + \sigma_{\mathbf{nn}}(\mathbf{v},q)\mathbf{n}\cdot\mathbf{u}) + \mathcal{H}_\beta\beta(\mathbf{t}\cdot\mathbf{u})(\mathbf{t}\cdot\mathbf{v}) + \mathcal{H}_{\mathcal{N}}\frac{\gamma_0}{h}(\mathbf{n}\cdot\mathbf{u})(\mathbf{n}\cdot\mathbf{v})\ \mathrm{d}s, \\ F_\Gamma &= \int_{\mathcal{E}_i} (1-\mathcal{H}_{\mathcal{N}})p_w\mathbf{n}\cdot\mathbf{v}\ \mathrm{d}s. \end{aligned} \tag{30}$$

A summary of the ~~discussion~~ numerical treatment of the GL is:

- Advance phase $\Rightarrow$ indicator χ in (27), case i or case ii
- Retreat phase $\Rightarrow$ indicator $\tilde{\chi}$ in (29), case ii

The case is determined by the geometry of the GL element and the sign of the indicator χ.

The algorithm for the GL element is:

Algorithm 3 Subgrid modeling for the GL element

Take all the 'potential GL elements' and solve $\chi(\mathbf{x}) = 0$ (advance phase) or $\tilde{\chi}(\mathbf{x}) = 0$ (retreat phase) to find $\tilde{x}_{GL}$ and the GL element.
Determine which case this GL element belongs to by checking the geometrical conditions at $\mathbf{x}_i$.
Specify $\mathcal{H}_\mathcal{N}(x)$ and $\mathcal{H}_\beta(x)$ based on $\tilde{x}_{GL}$ depending on the case and the advance or retreat phase.
Integrate Eq. (30) for the FEM matrix assembly.

Equations (1), (7), and (8) form a system of coupled nonlinear equations. They are solved in the same manner as in Elmer/ICE v.8.3. The detailed procedure is explained in Algorithms 1, 2, and 3. The solution to the nonlinear FS system is computed with Picard iterations to a 10^{-5} relative error with a limit of maximal 25 nonlinear iterations. The $\tilde{\mathbf{x}}_{GL}$ position is determined dynamically during each fixed-point iteration by solving Eq. (28) with χ or $\tilde{\chi}$ and the solution $\sigma_{\mathbf{nn}}(\mathbf{x})$ from the previous nonlinear iteration, and the step functions $\mathcal{H}_\mathcal{N}$ and $\mathcal{H}_\beta$ are adjusted accordingly.

The water pressure p_b is fixed since the ice geometry is not changed during the nonlinear iterations.

5 Results

The numerical experiments follow the MISMIP benchmark (Pattyn et al., 2012) and a comparison is made with the results in ~~(Gagliardini et al., 2016)~~Gagliardini et al. (2016). Using the experiment MISMIP 3a, the setups are exactly the same as in the advancing and retreating simulations in ~~(Gagliardini et al., 2016)~~Gagliardini et al. (2016). The experiments are run with spatial resolutions of $\Delta x = 4$ km, ~~2 kmand 1~~2 km, 1 km and 0.5 km. The mesh at the base is extruded vertically in 20 layers with equidistantly placed nodes in each vertical column. The ~~timestep~~ time step is $\Delta t = 0.125$ year for all ~~the three~~ four resolutions to eliminate time discretization errors when comparing different spatial resolutions.

The dependence on γ_0 in (30) for the retreating ice is shown in Fig. 4 with γ_0 between 10^4 and 10^9. The estimated GL positions do not vary with different choices of γ_0 from 10^5 to 10^8 which suggests a suitable range of γ_0. If γ_0 is too small ($\gamma_0 \ll 10^4$), oscillations appear in the estimated GL positions. If γ_0 is too large ($\gamma_0 \gg 10^8$), then more nonlinear iterations in Algorithm 1 are needed in each ~~timestep~~time step. The same dependency of γ_0 is observed for the ~~advance~~ advancing experiments and for different mesh resolutions as well. The results are not very sensitive to γ_0 and for the remaining experiments we choose $\gamma_0 = 10^6$.

The GL position during ~~10000 years~~ the transient simulations in the advance and retreat phases are displayed in Fig. 5 ~~for different mesh resolutions~~and the steady state results (at $t = 10000$) are shown in Fig. 6 for different mesh resolutions. The range of the ~~results from (Gagliardini et al., 2016) with $\Delta x = 25$ and 50 m~~ steady state solutions from Gagliardini et al. (2016) with mesh resolution from 25 m to 200 m are shown as background shaded regions ~~with colors purple and pink, respectively~~in red. We achieve similar GL migration results ~~both for~~ for both the advance and retreat experiments with at least 20 times larger ~~mesh resolutions.~~ mesh resolutions. The GL position is insensitive to the variation in mesh size between 0.5 km and 4 km. The distance between the steady state GL positions of the retreat and the advance phases is shown in Fig. 6 (b). The maximal

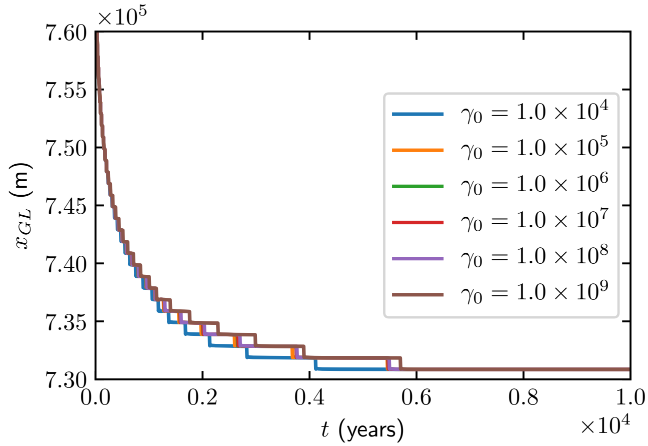

Figure 4. The MISMIP 3a retreat experiment with ~~$\Delta x = 1000$~~$\Delta x = 1$ ~~m~~ km for different choices of γ_0 in the time interval $[0, 10000]$ years.

distance is about 6 km at $\Delta x = 1$ km with the subgrid model, whereas in Gagliardini et al. (2016), the resolution has to be below 50 m to achieve a similar result.

We observed oscillations at the ice surface near the GL in all the experiments as expected from ~~(Durand et al., 2009a; Schoof, 2011)~~ Durand et al. (2009a); Schoof (2011). A zoom-in plot of the surface elevation with ~~$\Delta x = 1$~~$\Delta x = 0.5$ km at $t = 10000$ years is ~~shown~~ found to the left in Fig. 7, where the red dashed line indicates the estimated GL position. ~~Obviously, the estimated GL position does not coincide with any nodes even at the steady state.~~

The ratio between the thickness below sea level H_{bw} and the ice thickness H is shown to the right in Fig. 7. The horizontal, purple, dash-dotted line ~~indicates~~ represents the ratio of ρ/ρ_w and the estimated GL is located at the red, dashed line. This result confirms that the hydrostatic assumption $H\rho = H_{bw}\rho_w$ in Eq. (9) is not valid in the FS equations for $x > x_{GL}$ close to the GL and at the GL position, cf. ~~(Durand et al., 2009a; Schoof, 2011)~~Durand et al. (2009a); Schoof (2011). For $x < x_{GL}$ we have that $H_{bw}/H < \rho/\rho_w$ since H_{bw} decreases and H increases. The conclusion from numerical experiments in ~~(van Dongen et al., 2018)~~ van Dongen et al. (2018) is that the hydrostatic assumption and the SSA equations approximate the FS equations well for the floating ice beginning at a short distance away from the GL.

The solution varies smoothly over the mesh and $\Delta x = 0.5$ km appears to be a sufficient resolution in both panels of Fig. 7. In general, the estimated GL position does not coincide with any nodes even at the steady state but it may be close to a node. The surface and the base velocity solutions from the retreat experiment are displayed in Fig. 8 with ~~$\Delta x = 1$~~$\Delta x = 0.5$ km after 10000 years. The horizontal velocities on the two surfaces are similar with negligibly small differences on the floating ice as expected. The vertical velocities w on the surface (orange line) and the base (blue line) at the GL are almost discontinuous as analyzed in ~~(Schoof, 2011)~~Schoof (2011). With the subgrid model, the rapid variation is ~~represented on the 1~~ captured on the 0.5 km mesh size.

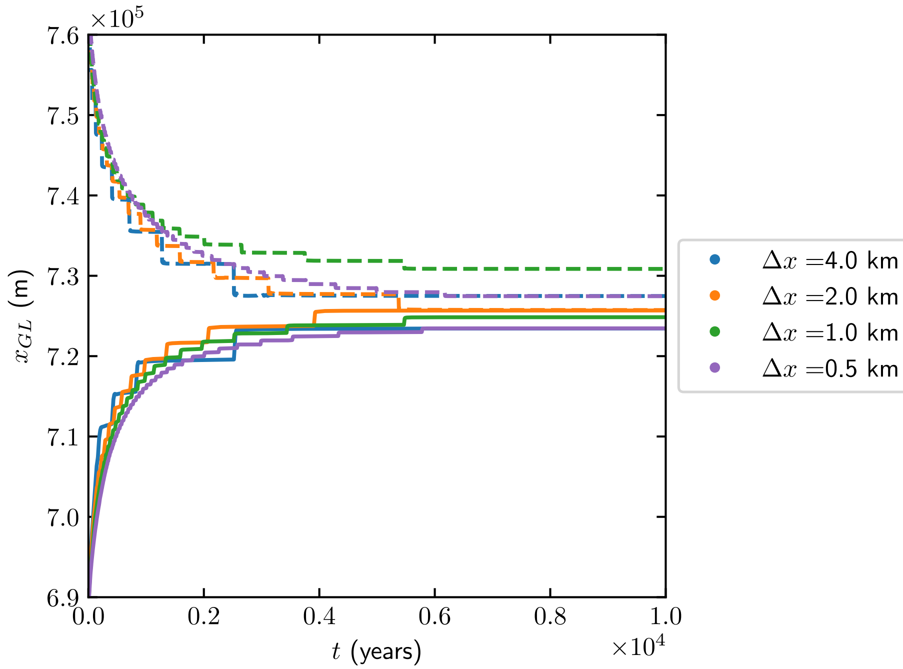

Figure 5. The MISMIP 3a experiments for the GL position when $t \in [0, 10000]$ with ~~$\Delta x = 4000, 2000$~~ $\Delta x = 4$ km, 2 km, 1 km and ~~1000~~0.5 ~~m~~ km for the advance (solid) and retreat (dashed) phases. ~~The shaded regions indicate the range of the results in (Gagliardini et al., 2016) with $\Delta x = 50$ m in red and $\Delta x = 25$ m in blue.~~

6 Discussion

~~Seroussi et al (Seroussi et al., 2014)~~ Seroussi et al. (2014) describe four different subgrid models (~~(~~NSEP, SEP1, SEP2 and SEP3) for the friction in SSA and evaluate them in a FEM discretization on a triangulated, planar domain. The ~~hydrostatic~~ flotation criterion is applied at the nodes of the triangles. In the NSEP, an element is floating or not depending on how many of the nodes that are floating. In the other three methods, an inner structure in the triangular element is introduced. One part of a triangle is floating and one part is grounded. The amount of friction in a triangle with the GL is determined by the flotation criterion. Either the friction coefficient is reduced, the integration in the element only includes the grounded part, or a higher order polynomial integration (SEP3) is applied. Faster convergence as the mesh is refined is observed for the latter methods compared to the first method. The discretization of the friction in Sect. 4 is similar to the SEP3 method but the FS equations also require a subgrid treatment of the normal velocity condition. In the method for the FS equations in ~~(Gagliardini et al., 2016)~~ Gagliardini et al. (2016), the GL position is in a node and the friction coefficient is approximated in three different ways. The coefficient is discontinuous at the node in one case (DI in ~~(Gagliardini et al., 2016)~~Gagliardini et al. (2016)). Our coefficient is also discontinuous but at the estimated location of the GL between the nodes.

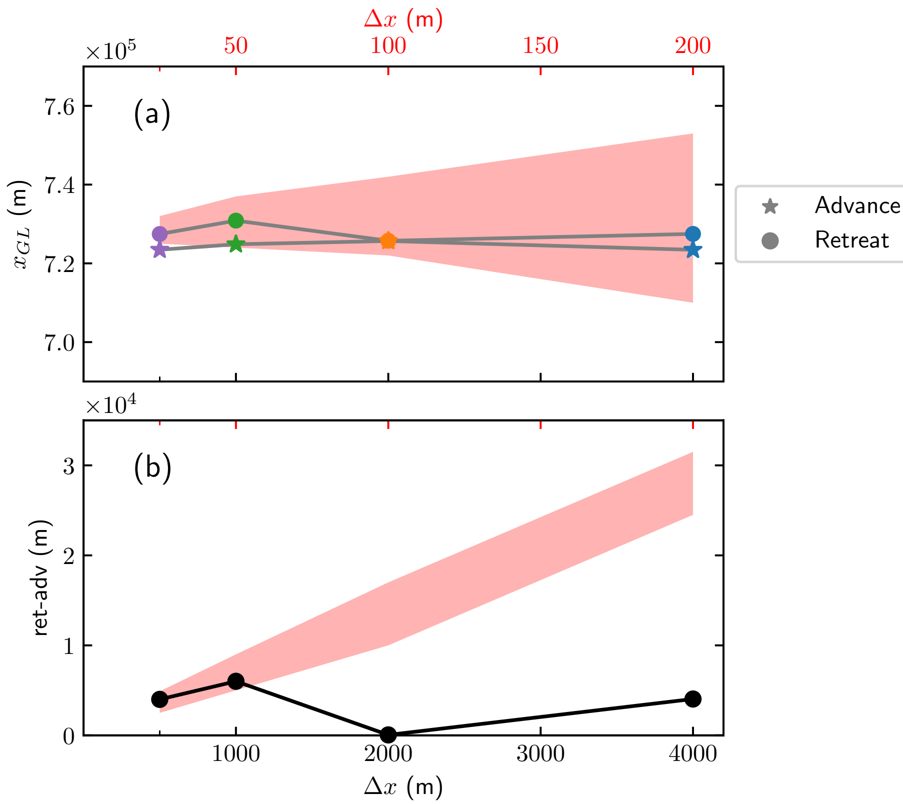

Figure 6. The MISMIP 3a experiments at the final time $t = 10000$ with the resolutions at $\Delta x = 4$ km, 2 km, 1 km and 0.5 km. (a) The GL positions in the advance (★) and retreat (●) phases. (b) The distance between the retreat and the advance x_{GL} at the steady states. The shaded regions indicate the range of the results in Gagliardini et al. (2016) with *20 times smaller mesh resolutions* from 25 to 200 m with the axis scale shown in red at the top of the plot.

The convergence of the steady state GL position toward the reference solutions in ~~(Gagliardini et al., 2016)~~ Gagliardini et al. (2016) is observed in the simulations in Fig. 5 and 6. However, as the meshes we used are ~~more than 40~~ at least 20 times larger than the 25 m finest resolution in ~~(Gagliardini et al., 2016)~~Gagliardini et al. (2016), it is still far from the convergence asymptote. At the current resolutions, the discretization introduces a strong mesh effect such as the two different geometrical interpretations in the two cases mentioned in Sect. 4. The subgrid scheme is able to provide a more accurate representation of the GL position and the boundary conditions, but the numerical solution of the velocity field, pressure as well as the two free surfaces are still ~~determined by~~ computed on the coarse mesh, which are the main sources of the numerical errors. Additional uncertainty at the GL is introduced by the approximation of the bedrock geometry, the friction at the GL, and the modeling of the ice/ocean interaction. It is shown in Cheng and Lötstedt (2020) that the solution at the GL is particularly sensitive to variation in the geometry and friction at the ice base. Our method can be extended to a triangular mesh covering Γ_b in the following way

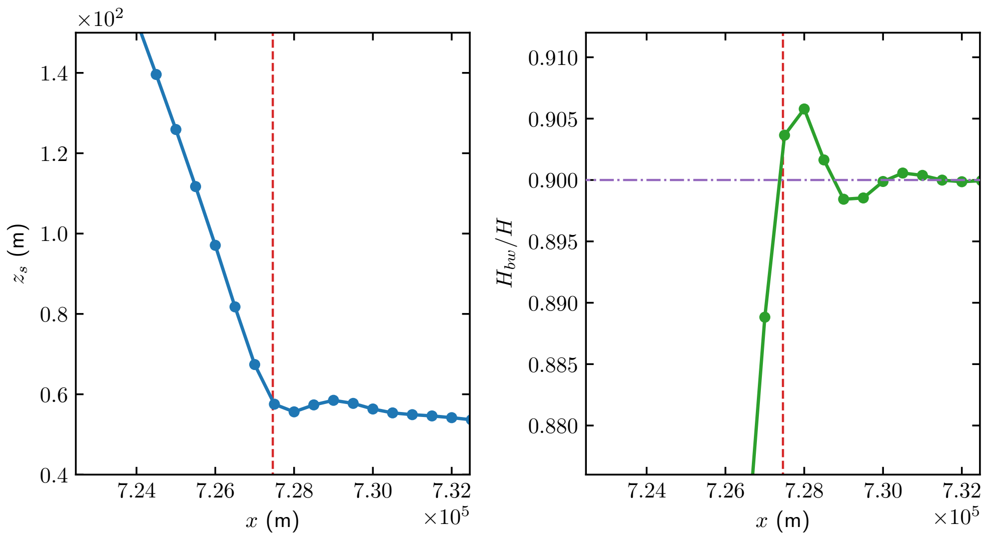

Figure 7. Details of the solutions for the retreat experiment with $\cancel{\Delta x = 1}$ $\Delta x = 0.5$ km after 10000 years. The solid dots represent the nodes of the elements and the vertical, red, dashed lines indicate the GL position. *Left panel*: The oscillations at ice surface near GL. *Right panel*: The flotation criterion is evaluated by H_{bw}/H. The ratio between ρ/ρ_w is drawn in a horizontal, purple, dash-dotted line.

(considering linear Lagrange functions). The condition on χ in Eq. (27) or $\tilde{\chi}$ in Eq. (29) is applied on the edges of each triangle $\mathcal{T}$ in the mesh. If $\cancel{\tilde{\chi} < 0}$ $\chi < 0$ in all three nodes then $\mathcal{T}$ is grounded. If $\cancel{\tilde{\chi} \geq 0}$ $\chi \geq 0$ in all nodes then $\mathcal{T}$ is floating. The GL passes inside $\mathcal{T}$ if $\cancel{\tilde{\chi}}$ χ has a different sign in one of the nodes. Then the GL crosses the two edges where $\cancel{\tilde{\chi} < 0}$ $\chi < 0$ in one node and $\cancel{\tilde{\chi} \geq 0}$ $\chi \geq 0$ in the other node. In this way, a continuous reconstruction of a piecewise linear GL is possible on Γ_b. The same tests are applied to $\tilde{\chi}$. The FEM approximation is modified in the same manner as in Sect. 4 using step functions in Nitsche's method.

An alternative to a subgrid scheme is to introduce static or dynamic adaptation of the mesh on Γ_b with a refinement at the GL as in e.g. ~~(Cornford et al., 2013; Drouet et al., 2013; Gladstone et al., 2010a)~~Gladstone et al. (2010a); Cornford et al. (2013); Drouet et al. . In general, a fine mesh is needed ~~along~~ at the GL and in an area surrounding it. Since the GL moves long distances ~~at least~~ in simulations of palaeo-ice sheets, the adaptation should be dynamic, permit refinement and coarsening of the mesh varying in time, and be based on some estimate of the numerical error of the method. In shorter time intervals, a static adaptation may be sufficient since the GL will move a shorter distance. Furthermore, shorter ~~timesteps~~ time steps are necessary for ~~stability when the mesh size is smaller in a mesh adaptive method.~~ numerical stability in static and dynamic mesh adaptation schemes. A static adaptation is determined once before the simulation starts. Introducing a time dependent, dynamic mesh adaptivity into an existing code requires a substantial coding effort and will increase the computational work considerably. Subgrid modeling is easier to implement and the increase in computing time is small. A combination of dynamic mesh adaptation and subgrid discretization may be the ultimate solution.

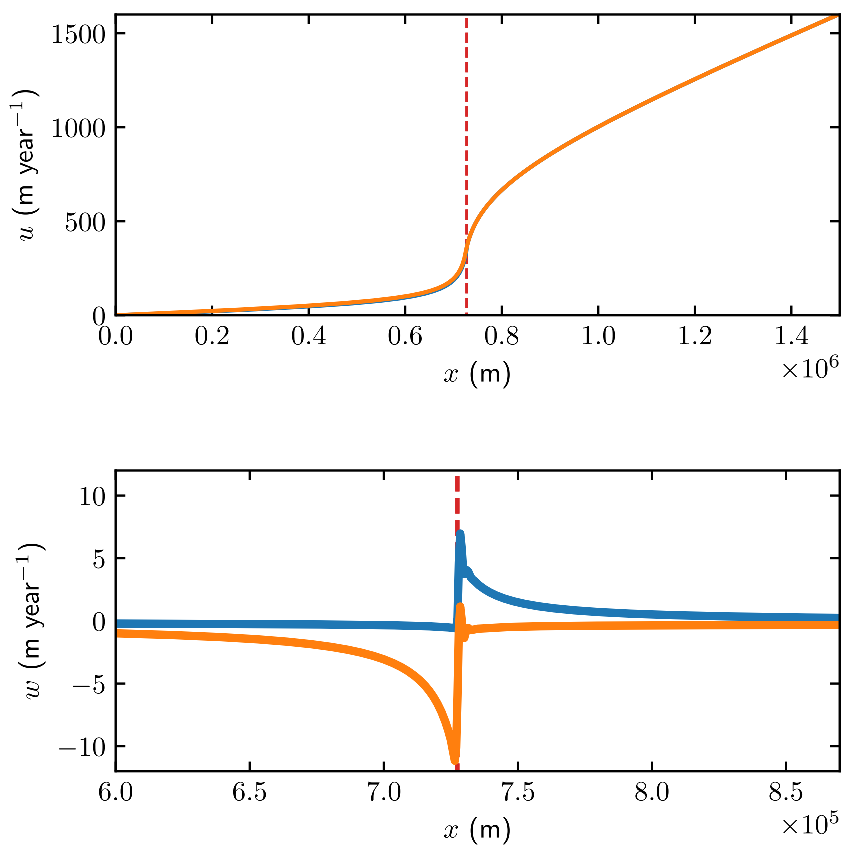

Figure 8. The velocities u (upper panel) and w (lower panel) on the surface (orange) and the base (blue) of the ice in the retreat experiment with ~~$\Delta x = 1$~~$\Delta x = 0.5$ km after 10000 years. The red, dashed line marks the GL position. The vertical velocity w is zoomed-in close to the GL.

7 Conclusions

A subgrid scheme at the GL has been developed and tested in the SSA model for 2D vertical ice flow in ~~(Gladstone et al., 2010b) and in (Seroussi et al., 2014)~~Gladstone et al. (2010b) and in Seroussi et al. (2014), for the friction in the vertically integrated model BISICLES (Cornford et al., 2013) for 2D flow in ~~(Cornford et al., 2016)~~Cornford et al. (2016), and for the PISM model mixing SIA with SSA in 3D in ~~(Feldmann et al., 2014)~~Feldmann et al. (2014). Here we propose a subgrid scheme for the FS equations for a 2D vertical ice, implemented in Elmer/ICE, that can be extended to 3D. The mesh is static and the moving GL position within one element is determined by linear interpolation with an auxiliary function $\chi(\mathbf{x})$ or $\tilde{\chi}(\mathbf{x})$. Only in that element, the FEM discretization is modified to accommodate the discontinuities in the boundary conditions.

The numerical scheme is applied to the simulation of a 2D vertical ice sheet with an advancing GL and one with a retreating GL. The model setups for the tests are the same as in one of the MISMIP examples (Pattyn et al., 2012) and in

~~(Gagliardini et al., 2016)~~Gagliardini et al. (2016). Comparable results to ~~(Gagliardini et al., 2016)~~ Gagliardini et al. (2016) are obtained using the subgrid scheme with more than 20 times larger mesh sizes. A larger mesh size also allows a longer ~~timestep~~ time step for the time integration. ~~Solving $\tilde{\chi}(\mathbf{x}) = 0$ for $\mathbf{x}_{GL}$ provides a good approximation of the GL position.~~

Code availability. The FS sub-grid model is implemented based on Elmer/ICE Version: 8.3 (Rev: f6bfdc9) with the scripts at http://doi.org/10.5281/zenodo.3401478 and http://doi.org/10.5281/zenodo.3401475.

Author contributions. GC developed the model code and performed the simulations. GC and PL contributed to the theory of the paper. GC, PL and LvS contributed to the development of the method and the writing of the paper

Competing interests. The authors declare that they have no conflict of interest.

Acknowledgements. This work has been supported by Nina Kirchner's Formas grant 2017-00665 and the Swedish e-Science initiative eSSENCE. We are grateful to Thomas Zwinger for advise and help in the implementation of the subgrid scheme in Elmer/ICE. The computations were performed on resources provided by the Swedish National Infrastructure for Computing (SNIC) at the PDC Center for High Performance Computing, KTH Royal Institute of Technology. We also thank the anonymous referees for their helpful comments.

References

Brondex, J., Gagliardini, O., Gillet-Chaulet, F., and Durand, G.: Sensitivity of grounding line dynamics to the choice of the friction law, J. Glaciology, 63, 854–866, 2017.

Chen, Q., Gunzburger, M., and Perego, M.: Well-posedness results for a nonlinear Stokes problem arising in glaciology, SIAM Journal on Mathematical Analysis, 45, 2710–2733, 2013.

Cheng, G. and Lötstedt, P.: Parameter sensitivity analysis of dynamic ice sheet models-numerical computations, Cryosphere, 14, 673–691, 2020.

Cheng, G., Lötstedt, P., and von Sydow, L.: Accurate and stable time stepping in ice sheet modeling, Journal of Computational Physics, 329, 29–47, 2017.

Chouly, F., Fabre, M., Hild, P., Mlika, R., Pousin, J., and Renard, Y.: An overview of recent results on Nitsche's method for contact problems, in: Geometrically unfitted finite element methods and applications, pp. 93–141, Springer, 2017a.

Chouly, F., Hild, P., Lleras, V., and Renard, Y.: Nitsche-based finite element method for contact with Coulomb friction, in: European Conference on Numerical Mathematics and Advanced Applications, pp. 839–847, Springer, 2017b.

Christensen, P. W., Klarbring, A., Pang, J. S., and Strömberg, N.: Formulation and comparison of algorithms for frictional contact problems, Int. J. Num. Meth. Eng., 42, 145–173, 1998.

Cornford, S., Martin, D., Lee, V., Payne, A., and Ng, E.: Adaptive mesh refinement versus subgrid friction interpolation in simulations of Antarctic ice dynamics, Ann. Glaciol., 57, 1–9, 2016.

Cornford, S. L., Martin, D. F., Graves, D. T., Ranken, D. F., Brocq, A. M. L., Gladstone, R. M., Payne, A. J., Ng, E. G., and Lipscomb, W. H.: Adaptive mesh, finite volume modeling of marine ice sheets, J. Comput. Phys., 232, 529–549, 2013.

DeConto, R. M. and Pollard, D.: Contribution of Antarctica to past and future sea-level rise, Nature, 531, 591–597, 2016.

Docquier, D., Perichon, L., and Pattyn, F.: Representing grounding line dynamics in numerical ice sheet models: Recent advances and outlook, Surv. Geophys., 32, 417–435, 2011.

van Dongen, E. C. H., Kirchner, N., van Gijzen, M. B., van de Wal, R. S. W., Zwinger, T., Cheng, G., Lötstedt, P., and von Sydow, L.: Dynamically coupling full Stokes and shallow shelf approximation for marine ice sheet flow using Elmer/ICE (v8. 3), Geoscientific Model Development, 11, 4563–4576, 2018.

Drouet, A. S., Docquier, D., Durand, G., Hindmarsh, R., Pattyn, F., Gagliardini, O., and Zwinger, T.: Grounding line transient response in marine ice sheet models, Cryosphere, 7, 395–406, 2013.

Durand, G. and Pattyn, F.: Reducing uncertainties in projections of Antarctic ice mass loss, Cryosphere, 9, 2043–2055, 2015.

Durand, G., Gagliardini, O., de Fleurian, B., Zwinger, T., and Le Meur, E.: Marine ice sheet dynamics: Hysteresis and neutral equilibrium, J. Geophys. Res.: Earth Surf., 114, F03 009, 2009a.

Durand, G., Gagliardini, O., Zwinger, T., Le Meur, E., and Hindmarsh, R. C. A.: Full Stokes modeling of marine ice sheets: influence of the grid size, Ann. Glaciol., 50, 109–114, 2009b.

Feldmann, J., Albrecht, T., Khroulev, C., Pattyn, F., and Levermann, A.: Resolution-dependent performance of grounding line motion in a shallow model compared with a full-Stokes model according to the MISMIP3d intercomparison, J. Glaciol., 60, 353–360, 2014.

Franca, L. P. and Frey, S. L.: Stabilized finite element methods: II. The incompressible Navier-Stokes equations, Computer Methods in Applied Mechanics and Engineering, 99, 209–233, 1992.

Gagliardini, O., Zwinger, T., Gillet-Chaulet, F., Durand, G., Favier, L., de Fleurian, B., Greve, R., Malinen, M., Martín, C., Råback, P., Ruokolainen, J., Sacchettini, M., Schäfer, M., Seddik, H., and Thies, J.: Capabilities and performance of Elmer/Ice, a new generation ice-sheet model, Geosci. Model Dev., 6, 1299–1318, 2013.

Gagliardini, O., Brondex, J., Gillet-Chaulet, F., Tavard, L., Peyraud, V., and Durand, G.: On the substantial influence of the treatment of friction at the grounding line, Cryosphere, 9, 3475–3501, 2015.

Gagliardini, O., Brondex, J., Gillet-Chaulet, F., Tavard, L., Peyaud, V., and Durand, G.: Impact of mesh resolution for MISMIP and MISMIP3d experiments using Elmer/ICE, The Cryosphere, 10, 307–312, 2016.

Gladstone, R. M., Lee, V., Vieli, A., and Payne, A. J.: Grounding line migration in an adaptive mesh ice sheet model, J. Geophys. Res., 115, F04 014, 2010a.

Gladstone, R. M., Payne, A. J., and Cornford, S. L.: Parameterising the grounding line in flow-line ice sheet models, Cryosphere, 4, 605–619, 2010b.

Gladstone, R. M., Warner, R. C., Galton-Fenzi, B. K., Gagliardini, O., Zwinger, T., and Greve, R.: Marine ice sheet model performance depends on basal sliding physics and sub-shelf melting, Cryosphere, 11, 319–329, 2017.

Gong, Y., Zwinger, T., Cornford, S., Gladstone, R., Schäfer, M., and Moore, J. C.: Importance of basal boundary conditions in transient simulations: case study of a surging marine-terminating glacier on Austfonna, Svalbard, J. Glaciol., 63, 106–117, 2017.

Hanna, E., Navarro, F. J., Pattyn, F., Domingues, C. M., Fettweis, X., Ivins, E. R., Nicholls, R. J., Ritz, C., Smith, B., Tulaczyk, S., Whitehouse, P. L., and Zwally, H. J.: Ice-sheet mass balance and climate change, Nature, 498, 51–59, 2013.

Helanow, C. and Ahlkrona, J.: Stabilized equal low-order finite elements in ice sheet modeling–accuracy and robustness, Computational Geosciences, 22, 951–974, 2018.

Hutter, K.: Theoretical Glaciology, D. Reidel Publishing Company, Terra Scientific Publishing Company, Dordrecht, 1983.

Jouvet, G. and Rappaz, J.: Analysis and finite element approximation of a nonlinear stationary Stokes problem arising in glaciology, Adv. Numer. Anal., 2011, 164 581, 2011.

Kingslake, J., Scherer, R. P., Albrecht, T., Coenen, J., Powell, R. D., Reese, R., Stansell, N. D., Tulaczyk, S., Wearing, M. G., and Whitehouse, P. L.: Extensive retreat and re-advance of the West Antarctic ice sheet during the Holocene, Nature, 558, 430–434, 2018.

Konrad, H., Shepherd, A., Gilbert, L., Hogg, A. E., McMillan, M., Muir, A., and Slater, T.: Net retreat of Antarctic glacier grounding line, Nat. Geosci., 11, 258–262, 2018.

Larour, E., Seroussi, H., Adhikari, S., Ivins, E., Caron, L., Morlighem, M., and Schlegel, N.: Slowdown in Antarctic mass loss from solid Earth and sea-level feedbacks, Science, 364, eaav7908, 2019.

Leguy, G. R., Asay-Davis, X. S., and Lipscomb, W. H.: Parameterization of basal friction near grounding lines in a one-dimensional ice sheet model, Cryosphere, 8, 1239–1259, 2014.

Leng, W., Ju, L., Gunzburger, M., Price, S., and Ringler, T.: A parallel high-order accurate finite element nonlinear Stokes ice sheet model and benchmark experiments, J. Geophys. Res.: Earth Surf., 117, 2156–2202, 2012.

MacAyeal, D. R.: Large-scale ice flow over a viscous basal sediment: Theory and application to Ice Stream B, Antarctica., J. Geophys. Res., 94, 4071–4078, 1989.

Martin, N. and Monnier, J.: Four-field finite element solver and sensitivities for quasi-Newtonian flows, SIAM Journal on Scientific Computing, 36, S132–S165, 2014.

Nitsche, J.: Über ein Variationsprinzip zur Lösung von Dirichlet-Problemen bei Verwendung von Teilräumen, die keinen Randbedingungen unterworfen sind, Abh. Math. Semin., University of Hamburg, Germany, 36, 9–15, 1971.

Nowicki, S. M. J. and Wingham, D. J.: Conditions for a steady ice sheet–ice shelf junction, Earth Plan. Sci. Lett., 265, 246–255, 2008.

Pattyn, F. and Durand, G.: Why marine ice sheet model predictions may diverge in estimating future sea level rise, Geophys. Res. Lett., 40, 4316–4320, 2013.

Pattyn, F., Schoof, C., Perichon, L., Hindmarsh, R. C. A., Bueler, E., de Fleurian, B., Durand, G., Gagliardini, O., Gladstone, R., Goldberg, D., Gudmundsson, G. H., Huybrechts, P., Lee, V., Nick, F. M., Payne, A. J., Pollard, D., Rybak, O., Saito, F., and Vieli, A.: Results of the Marine Ice Sheet Model Intercomparison Project, MISMIP, Cryosphere, 6, 573–588, 2012.

Pattyn, F., Perichon, L., Durand, G., Favier, L., Gagliardini, O., Hindmarsh, R. C. A., Zwinger, T., Albrecht, T., Cornford, S., Docquier, D., Fürst, J. J., Goldberg, D., Gudmundsson, G. H., Humbert, A., Hütten, M., Jouvet, G., Kleiner, T., Larour, E., Martin, D., Morlighem, M., Payne, A. J., Pollard, D., Rückamp, M., Rybak, O., Seroussi, H., Thoma, M., and Wilkens, N.: Grounding-line migration in plan-view marine ice-sheet models: results of the ice2sea MISMIP3d intercomparison, J. Glaciol., 59, 410–422, 2013.

Reusken, A., Xu, X., and Zhang, L.: Finite element methods for a class of continuum models for immiscible flows with moving contact lines, Int. J. Numer. Meth. Fluids, 84, 268–291, 2017.

Schoof, C.: Marine ice sheet dynamics. Part 2. A Stokes flow contact problem, J. Fluid Mech., 679, 122–155, 2011.

Schoof, C. and Hindmarsh, R.: Thin-Film Flows with Wall Slip: An Asymptotic Analysis of Higher Order Glacier Flow Models, Quart. J. Mech. Appl. Math., 63, 73–114, 2010.

Seroussi, H., Morlighem, M., Larour, E., Rignot, E., and Khazendar, A.: Hydrostatic grounding line parameterization in ice sheet models, Cryosphere, 8, 2075–2087, 2014.

Stokes, C. R., Tarasov, L., Blomdin, R., Cronin, T. M., Fisher, T. G., Gyllencreutz, R., Hättestrand, C., Heyman, J., Hindmarsh, R. C. A., Hughes, A. L. C., Jakobsson, M., Kirchner, N., Livingstone, S. J., Margold, M., Murton, J. B., Noormets, R., Peltier, W. R., Peteet, D. M., Piper, D. J. W., Preusser, F., Renssen, H., Roberts, D. H., Roche, D. M., Saint-Ange, F., and Stroeven, A. P.: On the reconstruction of palaeo-ice sheets: Recent advances and future challenges, Quat. Sci. Rev., 125, 15–49, 2015.

Urquiza, J. M., Garon, A., and Farinas, M.-I.: Weak imposition of the slip boundary condition on curved boundaries for Stokes flow, J. Comput. Phys., 256, 748–767, 2014.

Wilchinsky, A. V. and Chugunov, V. A.: Ice-stream–ice-shelf transition: theoretical analysis of two-dimensional flow, Ann. Glaciology, 30, 153–162, 2000.

Zhang, T., Price, S., Ju, L., Lei, W., Brondex, J., Durand, G., and Gagliardini, O.: A comparison of two Stokes ice sheet models applied to the Marine Ice Sheet Model Intercomparison Project for plan view models, Cryosphere, 11, 179–190, 2017.